J. Fluid Mech. (2013), *vol.* 718, *pp.* 210–245.
doi:10.1017/jfm.2012.606

The role of wake stiffness on the wake-induced vibration of the downstream cylinder of a tandem pair

G. R. S. Assi[1,†], P. W. Bearman[2], B. S. Carmo[3], J. R. Meneghini[3], S. J. Sherwin[2] and R. H. J. Willden[4]

[1]Department of Naval Architecture and Ocean Engineering, University of São Paulo, São Paulo, 05508-030, Brazil

[2]Department of Aeronautics, Imperial College, London SW7 2AZ, UK

[3]Department of Mechanical Engineering, University of São Paulo, São Paulo, 05508-030, Brazil

[4]Department of Engineering Science, University of Oxford, Oxford OX1 3PJ, UK

(Received 22 March 2012; revised 23 October 2012; accepted 3 December 2012; first published online 8 February 2013)

When a pair of tandem cylinders is immersed in a flow the downstream cylinder can be excited into wake-induced vibrations (WIV) due to the interaction with vortices coming from the upstream cylinder. Assi, Bearman & Meneghini (*J. Fluid Mech.*, vol. 661, 2010, pp. 365–401) concluded that the WIV excitation mechanism has its origin in the unsteady vortex–structure interaction encountered by the cylinder as it oscillates across the wake. In the present paper we investigate how the cylinder responds to that excitation, characterising the amplitude and frequency of response and its dependency on other parameters of the system. We introduce the concept of *wake stiffness*, a fluid dynamic effect that can be associated, to a first approximation, with a linear spring with stiffness proportional to *Re* and to the steady lift force occurring for staggered cylinders. By a series of experiments with a cylinder mounted on a base without springs we verify that such wake stiffness is not only strong enough to sustain oscillatory motion, but can also dominate over the structural stiffness of the system. We conclude that while unsteady vortex–structure interactions provide the energy input to sustain the vibrations, it is the wake stiffness phenomenon that defines the character of the WIV response.

Key words: flow-structure interactions, vortex streets, wakes/jets

1. Introduction

Wake-induced vibration (WIV) is a fluid-elastic mechanism able to excite into transverse oscillatory motion a bluff body immersed in a wake generated from another body positioned upstream. In the present study we are concerned with the WIV of the downstream cylinder of a tandem pair. WIV differs from the well-studied phenomenon of *vortex-induced vibration* (VIV) in the sense that the excitation is not

† Present address: NDF Research Group, Dept. Eng. Naval e Oceânica, Escola Politécnica da Universidade de São Paulo, Av. Professor Mello Moraes 2231, 05508-030, São Paulo, SP, Brazil. Email address for correspondence: g.assi@usp.br

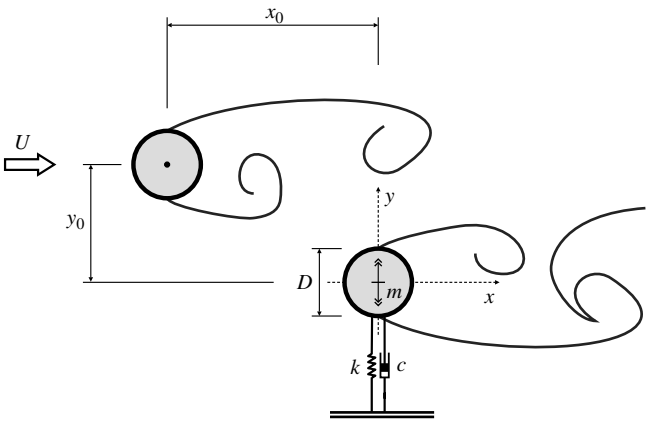

FIGURE 1. Arrangement of a pair of cylinders. The static upstream cylinder may be removed during experiments with a single cylinder. Solid lines represent hypothetical interaction between shear layers.

generated in the vortex shedding mechanism of the body itself, but it comes from the interaction with a wake developed farther upstream. In addition to that, while VIV is a resonant phenomenon, WIV does not depend on the fluid excitation matching the natural frequency of the structure. This will be explained in detail later.

In the past literature, WIV has also been referred to as: 'interference galloping' (Ruscheweyh 1983), 'wake-induced galloping' (Bokaian & Geoola 1984) and 'wake-displacement excitation' (Zdravkovich 1988). Nevertheless, later in the present work it will become clear why we hold to the WIV terminology.

In order to investigate the fundamental physics behind the phenomenon we study the simplest case consisting of two circular cylinders with the same diameter initially aligned with the flow. The basic arrangement is illustrated in figure 1, where x_0 and y_0 define the initial geometry of the pair. In the present work, the upstream cylinder is always static while the downstream cylinder is allowed to respond with oscillations in one degree of freedom (1-dof) in the cross-flow direction only.

Previous works found that the typical WIV response is characterized by an asymptotic build-up of amplitude with increasing reduced velocity. In one of them, Assi, Bearman & Meneghini (2010) investigated the origin of the fluid force involved in the excitation of the second cylinder. It has been concluded that WIV is indeed a wake-dependent type of *flow-induced vibration* (FIV), yet it was found that the unsteadiness of the wake plays a critical role in the WIV excitation mechanism and not simply the displacement of a steady flow field. It has been suggested that the WIV mechanism is sustained by unsteady vortex–structure interactions that input energy into the system as the downstream cylinder oscillates across the upstream wake. It has been shown that, in WIV, the upstream static body sheds vortices as an isolated cylinder while the downstream elastic body responds with oscillations at a different frequency. For flow velocities far beyond the typical VIV resonance the upstream vortex shedding frequency (f_s) can be many times the natural frequency (f_0), and yet the body will respond with severe vibrations.

Assi *et al.* (2010) showed that WIV is not a resonant phenomenon. Coherent vortices impinging on the second cylinder and merging with its own vortices induce fluctuations in lift that are not synchronized with the motion. While VIV finds

its maximum amplitude of vibration at the resonance when $f_s \approx f_0$, WIV response keeps increasing even when f_s is much higher than f_0. Nonetheless, for the sake of classification, WIV is essentially a type of vortex-induced mechanism in the sense that it requires the interaction of the structure with vortices, even though these vortices are coming from an upstream wake.

So far, this is what is known from previous research efforts as recently highlighted in Assi *et al.* (2010). In the present paper we will concentrate our attention on what we call the 'character' of the vibration. In other words, once we have understood why vibrations are excited and sustained (Assi *et al.* 2010), we are able to investigate how the cylinder responds to that excitation. Our objective is to characterize the response (amplitude and frequency) and its dependence on other parameters of the system, such as Reynolds number, x_0 separation, structural stiffness and structural damping. Thus, the present paper is a continuation of the work presented in Assi *et al.* (2010).

1.1. *WIV response of the downstream cylinder*

Reflecting a need from the heat-exchanger industry, the earliest experiments to measure the response due to WIV of a pair of cylinders were performed with flexible tubes in order to supply data to design engineers. A more complete understanding of the fluid mechanics of the phenomenon was gradually developed when researchers started to limit the number of variables, performing tests with rigid cylinders in 2-dof. A further step was to simplify even more and allow a rigid cylinder only to vibrate either in the in-line or in the cross-flow direction. First, let us present some previous data found in the literature (including figures reproduced in this paper) that will be useful to support our conclusions.

King & Johns (1976) performed experiments in water ($Re = 10^3$–2×10^4) with two flexible cylinders for separations in the range $x_0/D = 0.25$–6.0. They observed that for $x_0/D = 5.5$ the upstream cylinder responded with a typical VIV curve reaching amplitudes around $\hat{y}/D = 0.45$ at the resonance peak, comparable to their tests with a single cylinder at same Re. On the other hand the downstream cylinder also started to build up oscillations together with the upstream one, but instead of the oscillations disappearing after the synchronization range they remained at roughly the same level for reduced velocities up to the highest tested. They identified the response of the second cylinder as a type of buffeting, since it originated from the wake interference coming from the upstream cylinder.

Brika & Laneville (1999) performed tests with a pair of long tubes in a wind tunnel with a flexible cylinder positioned from 7 to 25 diameters downstream of a rigid cylinder for Reynolds number between 5000 and 27 000. A series of curves for different separations reveal that as x_0 increases the interference effect from the upstream wake is reduced until the response resembles that of a single cylinder without any (or with very little) interference. It is interesting to note that even between separations of 16 and 25 diameters the authors were still able to identify some change in the interference effect with the second cylinder positioned so far downstream. Because their experiment was performed in air, the mass ratio m^* (the ratio between the mass of the structure and the mass of displaced fluid) was two orders of magnitude higher than other experiments in water. Yet their damping parameter ζ was extremely low, resulting in a combined mass-damping of only $m^*\zeta = 0.068$.

Moving from flexible to rigid cylinders, we recall experiments performed by Zdravkovich (1985) with two rigid cylinders free to respond in 2-dof mounted in a wind tunnel ($Re = 1.5 \times 10^4$–9.5×10^4, $m^* = 725$ and $\zeta = 0.07$). Due to a very high mass-damping parameter of $m^*\zeta = 50$, Zdravkovich was only able to observe

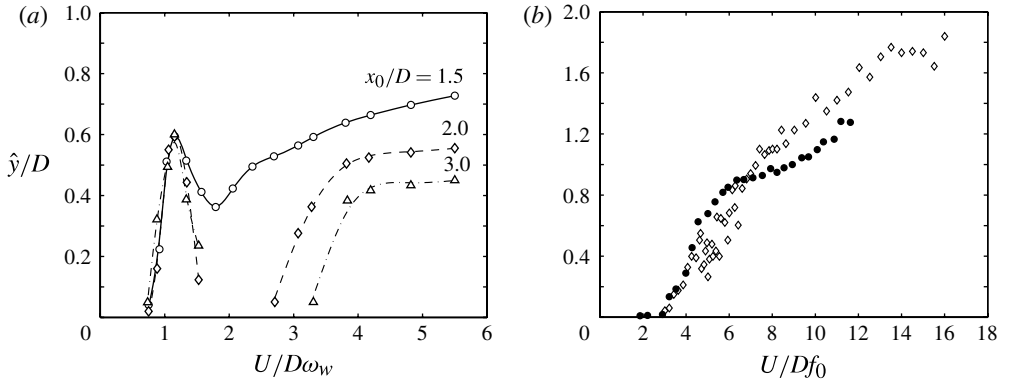

FIGURE 2. Response in the cross-flow direction of the downstream cylinder under WIV. (*a*) Varying x_0, $m^* = 8.4$, $\zeta = 0.013$, $Re = 700$–2000, ω_w is the natural frequency in radians per second measured in still water (Bokaian & Geoola 1984). (*b*) ◊, $x_0/D = 4.75$, $m^* = 3.0$, $\zeta = 0.04$, $Re = 3 \times 10^4$ (Hover & Triantafyllou 2001); ○, $x_0/D = 4.0$, $m^* = 1.9$, $\zeta = 0.007$, $Re = 3000$–$13\,000$ (Assi *et al.* 2006).

a build-up of oscillations at $x_0/D = 4.0$ for reduced velocities beyond $U/Df_0 = 50$, asymptotically reaching a maximum of $\hat{y}/D = 1.7$ for the last point of his experiments at around reduced velocity 80. Nevertheless, he has also recorded a monotonically increasing branch of response that was qualitatively very similar to those results later presented by Brika & Laneville (1999). In a subsequent study of the effect of mass and damping, Zdravkovich & Medeiros (1991) performed similar 2-dof tests in a wind tunnel varying $m^*\zeta$ between 6 and 200 ($Re = 5 \times 10^3$–1.4×10^5). Once more, the cross-flow vibrations presented the same monotonic-asymptotic behaviour with the amplitude increasing with the reduced velocity. Their results revealed a strong dependence of the response on $m^*\zeta$, but more importantly showed that very high values of mass-damping are required to inhibit WIV of the second cylinder. Maximum amplitude was obtained at a maximum reduced velocity of 120, but in order to reduce the amplitude $\hat{y}/D$ by half (from 2.2 to 1.1) it was required to increase $m^*\zeta$ ten times (from 6.4 to 64).

Going one step further in the simplification of the problem, we find a few results from Bokaian & Geoola (1984) who performed experiments for two rigid cylinders in tandem responding only in 1-dof in a water channel. The upstream cylinder was fixed while the downstream cylinder was elastically mounted on air bearings and free to respond only in the cross-flow direction. They varied centre-to-centre separation in the range of $x_0/D = 1.09$–5.0. Results for amplitude of response versus reduced velocity (with ω_w being the natural frequency in radians per second measured in still water) are presented in figure 2(*a*) for three values of x_0 tested. A vigorous build-up of oscillations with increasing flow speed is observed for all flow speeds greater than a critical threshold velocity. Such a severe 1-dof vibration was observed to resemble the response of classical galloping of non-circular bodies; therefore it was referred to as 'wake-induced galloping'. They noted that 'galloping carries the strong connotation of a negatively damped single degree of freedom oscillation, and its use to describe the problem under study is only because of the many similarities between the two kinds of instability'. However, elsewhere in their work Bokaian & Geoola (1984) stated that 'whilst some characteristics of *wake-excited galloping* were found to be similar to those of galloping of sharp-edged bodies, others were observed to be fundamentally

different'. The authors concluded that depending on x_0, m^* and ζ the downstream cylinder 'exhibited a vortex-resonance, or a galloping, or a combined vortex-resonance and galloping, or a separated vortex-resonance and galloping' response. In figure 2(*a*) two examples of these different responses are found: results for $x_0/D = 1.5$ present a vortex resonance that is followed by (or combined with) a 'galloping' response at about reduced velocity 2; results for $x_0/D = 2.0$ and 3.0 present separated vortex-resonance and 'galloping' regimes. A pure vortex resonance is not shown in figure 2(*a*) but this would be similar to what we understand as a typical VIV response.

Hover & Triantafyllou (2001) measured displacements of and forces on rigid cylinders under WIV in a water towing tank at a constant Reynolds number. They made use of a closed-loop control system that forces the oscillation of the cylinder in response to a measured and integrated fluid force. In this way they cleverly tuned the mass, damping and stiffness parameters (m–c–k) in an equation of motion in order to generate any artificial combination of f_0, m^* and ζ. As a result, their curve presented in figure 2(*b*) was obtained for $Re = 3 \times 10^4$ adjusting f_0 in order to vary the reduced velocity from 3 to 12. The resulting parameter $m^*\zeta = 0.12$ is very close to $m^*\zeta = 0.11$ obtained by Bokaian & Geoola (1984) in figure 2(*a*); however the difference in the level of amplitude might be related to a difference of one order of magnitude in Re, as will be discussed later. For a separation of $x_0/D = 4.75$, Hover & Triantafyllou (2001) observed one single branch of response that builds up monotonically reaching amplitudes of $[\hat{y}/D]_{max} = 1.9$ for reduced velocities around 17 (their curve represents an average of the 10 % highest peaks of displacement). Although they referred to the branch of high amplitude as an 'upward extension of the frequency lock-in branch' that occurs for the VIV response of a single cylinder, there is no evidence that the vortex shedding frequency of either cylinder is synchronized with the frequency of oscillation; on the contrary, their results reveal that vibrations occur 'without any clear signature of vortex resonance'.

More recently, Assi *et al.* (2006) performed 1-dof experiments with two rigid cylinders in a recirculating water channel ($Re = 3 \times 10^3$–1.3×10^4). Their results, also presented in figure 2(*b*), are comparable to those of Hover & Triantafyllou (2001) since they have a similar Re range; however Assi *et al.* (2006) employed a very low-damping elastic system resulting in $m^*\zeta = 0.013$, one order of magnitude lower. Both curves are in good agreement showing an expected branch of high-amplitude oscillation building up as the reduced velocity is increased. In addition, the data points from Assi *et al.* (2006) also reveal a smooth hump corresponding to a local vortex-resonance response around $U/Df_0 = 6.0$.

Later in this paper we shall return to some of these results in order to compare our data and support our conclusions.

1.2. *Steady fluid forces on staggered cylinders*

It is known that the downstream cylinder of a staggered pair experiences a steady lift force even if the bodies are held static in the flow (Price 1976; Bokaian & Geoola 1984). Zdravkovich (1977) presents a map of steady fluid forces acting on a cylinder across the wake for separations as large as $x_0/D = 5.0$. His results, which are in agreement with many other maps in the literature, clearly show that the steady lift always points towards the centreline of the wake, i.e. as restoring the staggered downstream cylinder back to the tandem configuration. The steady lift is zero on the centreline of the wake, increases as the second cylinder is displaced towards the wake interference boundary and is reduced as the body is positioned farther out of the wake. Assi *et al.* (2010) have suggested that such a strong steady lift is induced

by the unsteady interaction of vortices present in the wake coming from the upstream cylinder. In a controlled experiment, the periodic unsteadiness associated with vortex shedding was removed from the upstream wake, leaving only a steady shear profile generated by a set of screens. It was shown that the steady lift acting on a static downstream cylinder was considerably reduced if coherent vortices were not present in the upstream wake.

Igarashi (1981) and others have identified two distinct regimes in the wake formed in the gap between tandem cylinders. The first regime occurs when the proximity of the cylinders allows the shear layers that separate from the upstream cylinder to reattach to the second body and a vortex street is not developed in the gap. The second regime, which normally occurs for larger separations, is characterized by the existence of a developed vortex wake in the gap. The force map presented by Zdravkovich (1977) shows that distinct regimes also appear for staggered arrangements and a steady lift force presents two prominent regions associated with different wake regimes. In the present work we are only interested in the second regime, i.e. the force field and vibration generated when a developed wake is present in the gap. The transition from the first to the second regime has a small influence of Re, but most of the investigations agree that the critical separation is between $x_0/D = 3.0$ and 4.0.

Bokaian & Geoola (1984) presented more detailed measurements of the steady lift $\overline{C}_y$ acting across the wake for three separations of 3.0, 4.0 and 5.0 diameters and $Re = 5900$. Their measurements made it clear that the maximum lift towards the centreline decreases as the second cylinder moves farther downstream. While the steady drag $\overline{C}_x$ is minimum on the centreline, due to the shielding effect of the upstream wake, $\overline{C}_y$ is minimum around $y_0/D = 1.0$. This brings us back to the definition of interference regions proposed by Zdravkovich (1977). He says that 'the wake boundary is a line along which the (mean) velocity becomes the same as the free stream one. The (wake) interference boundary is the line along which (the mean) lift force becomes zero or negligible'. These two lines do not necessarily coincide, but the wake interference boundary is always outside the wake boundary. It will become clearer later that the interaction between flow and structure occurring within the wake boundary is fundamental to WIV.

1.3. *Vortex-induced vibration of a single cylinder*

Before starting our analysis of WIV, we briefly review the modelling employed to understand other types of flow-induced vibrations, especially vortex-induced vibration (VIV), which has its origin in the cyclic loads generated by vortices shed from a bluff body. It has been extensively reviewed in the literature (Sarpkaya 1979; Bearman 1984; Parkinson 1989; Blevins 1990; Zdravkovich 1997; Williamson & Govardhan 2004), but some of the basic modelling is mentioned here since it will be employed to model WIV later in this paper.

An elastic cylinder will be modelled by its structural properties: mass (m), stiffness (k) and damping (c). Allowing for displacements only in one degree of freedom (1-dof) in the y-axis, the equation of motion per unit length becomes

$$m\ddot{y} + c\dot{y} + ky = \tfrac{1}{2}\rho U^2 D\left[\overline{C}_y + \hat{C}_y \sin(2\pi ft + \phi)\right], \tag{1.1}$$

where y, $\dot{y}$ and $\ddot{y}$ are respectively the displacement, velocity and acceleration of the body, leaving the term on the right-hand side of the equation to represent the time-dependent fluid force in the cross-flow direction. As proposed by Bearman (1984) and others, the displacement of a cylinder under VIV may be expressed by the harmonic

response

$$y(t) = \hat{y}\sin(2\pi ft), \tag{1.2}$$

where $\hat{y}$ and f represent the harmonic amplitude and frequency of oscillation. For large-amplitude oscillation under a steady-state regime of VIV the fluid force and the body response oscillate at the same frequency f, which is usually close to the natural frequency of the system. According to this 'harmonic forcing and harmonic motion' hypothesis the fluid force can be divided into a time-average term $\overline{C}_y$ and a transient term modelled as a sine wave with amplitude $\hat{C}_y$ and frequency f. For body excitation to occur, the phase angle between $y(t)$ and $C_y(t)$ must be between $\phi = 0$ and 180°.

A second-order oscillator presents an undamped natural frequency that only takes into account the structural stiffness and mass of the system ($f_0 = \sqrt{k/4\pi^2 m}$). The structural damping is generally expressed by a damping ratio ζ, defined as a fraction of the critical damping ($\zeta = c/\sqrt{4km}$). If ζ is kept sufficiently low, the damped natural frequency can be considered approximately equal to f_0. It is useful to present the flow speed in terms of a reduced velocity U/Df_0. The reduced velocity for maximum VIV response occurs around U/Df_s (the inverse of the Strouhal number), that is at the resonance where the vortex shedding frequency f_s is equal to f_0.

According to Bearman (1984) the VIV response is inversely proportional to the product of m^* and ζ, yielding the non-dimensional amplitude of vibration as

$$\frac{\hat{y}}{D} = \frac{1}{4\pi^3}\hat{C}_y \sin\phi \left(\frac{U}{Df_0}\right)^2 \left(\frac{1}{m^*\zeta}\right)\left(\frac{f_0}{f}\right). \tag{1.3}$$

Bearman (1984) states that 'It is clear that the phase angle ϕ plays an extremely important role. The amplitude response does not depend on $\hat{C}_y$ alone but on that part of $\hat{C}_y$ in phase with the body velocity. Hence, measurements of just the sectional fluctuating lift coefficient on a range of stationary bluff-body shapes will give little indication of the likely amplitudes of motion of similar bodies flexibly mounted'. Therefore, the combined $\hat{C}_y \sin\phi$ term is fundamental in an unsteady analysis of the phenomenon.

2. Experimental set-up and validation with a single cylinder

The experimental set-up employed in the present study is exactly the same as that described in Assi *et al.* (2010). For further details, refer to Assi (2009). It is worth recalling here that a pair of coil springs connecting the moving base to the fixed supports provided the restoration force of the system. All the moving parts of the elastic base contributed to the effective mass oscillating along with the cylinder resulting in a mass ratio of $m^* = 2.6$ (calculated as the total oscillating mass divided by the mass of water displaced by the cylinder). By carrying out free decay tests in air it was also possible to estimate the structural damping of the system as $\zeta = 0.7\,\%$, calculated as a percentage of the critical damping. Therefore, the mass-damping parameter was $m^*\zeta = 0.018$ for the majority of the experiments.

In order to validate the experimental set-up and obtain reference data for comparison, a preliminary experiment was performed with a single cylinder free to oscillate in 1-dof in a uniform flow. These results have been discussed in more detail in Assi *et al.* (2010); therefore they will be presented very briefly here to allow comparison with the main WIV data to be discussed later.

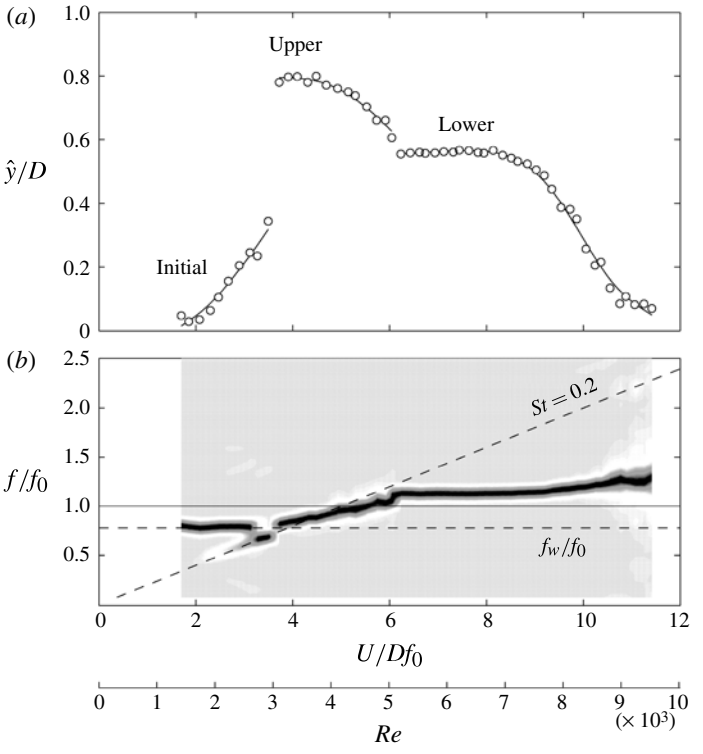

FIGURE 3. VIV response of a single cylinder free to oscillate in the cross-flow direction. Reproduced from Assi *et al.* (2010).

The typical VIV response, in terms of amplitude and frequency of oscillation, is presented in figure 3 and shows a good agreement with the results reviewed by Williamson & Govardhan (2004). The three typical branches of response, *initial*, *upper* and *lower*, are clearly identified in the displacement curve. Fluid force measurements (not presented in this paper) were in good agreement with the results presented by Khalak & Williamson (1999) and can be found in Assi *et al.* (2010). Figure 3 also shows the frequency response normalized by the natural frequency (f/f_0); variation from light to dark grey represents higher peaks in the normalized power spectral density (PSD) of the frequency of oscillation (refer to Assi 2009 for more details). (The f_w/f_0 line will be explained later.)

Throughout the study, the cylinder displacement amplitude normalized by the cylinder diameter ($\hat{y}/D$) was found by measuring the r.m.s. value of response and multiplying by $\sqrt{2}$. Such a harmonic amplitude assumption is likely to give an underestimation of maximum response but was judged to be perfectly acceptable for assessing the average amplitude of response for many cycles of steady-state oscillations. The same procedure was employed to determine the magnitude of all other fluctuating variables, such as $\hat{C}_y$ and $\hat{C}_x$.

3. Results: WIV response of the downstream cylinder

The characteristic build-up of response for higher reduced velocities, reported in previous works, is clearly observed in figure 4 and contrasts with the typical VIV

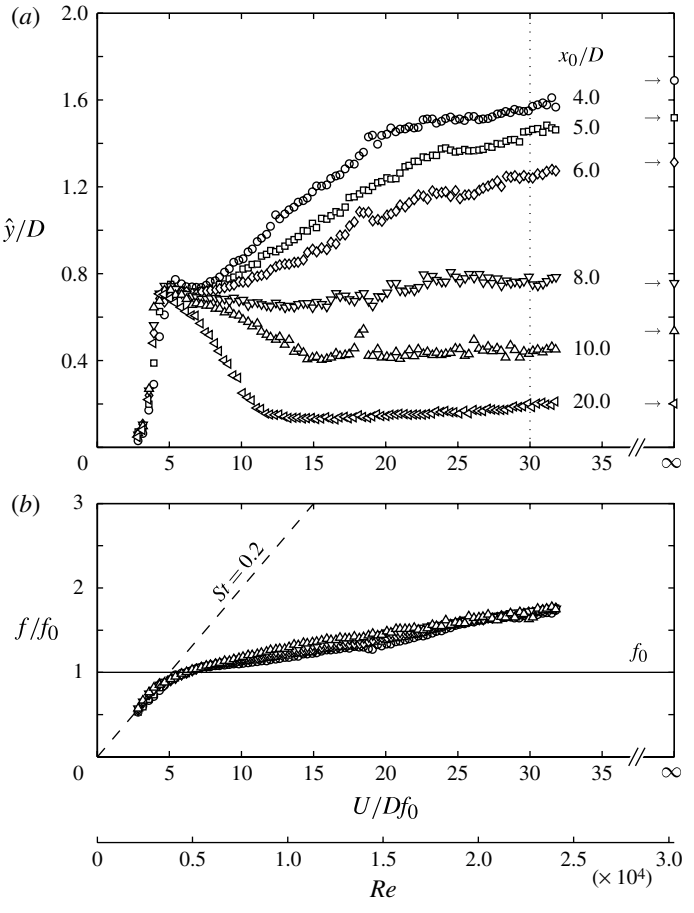

FIGURE 4. WIV response of the downstream cylinder for various x_0 separations: (*a*) displacement; (*b*) dominant frequency of oscillation.

response obtained for a single cylinder in figure 3. A discrete hump is found to occur for all centre-to-centre separations at around $U/Df_0 = 5.0$ and corresponds to the local peak of VIV resonance, although this happens slightly later in the reduced velocity scale due to the shielding effect of the wake that reaches the downstream cylinder. Beyond that, for higher reduced velocities, a branch of monotonically increasing amplitude starts to build up showing different levels of vibration for each separation. As expected, it reveals that displacement amplitude is inversely proportional to the separation x_0. As the downstream cylinder is moved farther away, the effect of WIV is reduced until the response curve eventually resembles that of VIV of an isolated cylinder. While at $x_0/D = 4.0$ the cylinder reaches displacement amplitudes around $\hat{y}/D = 1.6$, a cylinder at $x_0/D = 20$ shows only the VIV peak with levels of $\hat{y}/D$ around 0.2 for the rest of the regime. The curve for $x_0/D = 8.0$ is a particularly interesting one because the intensity of the WIV effect is just enough to sustain the same level of response observed for VIV through the whole range of reduced velocities. Nevertheless, all presented cases show some type of combined VIV and WIV response, with the maximum amplitude of VIV at $U/Df_0 = 5.0$ showing a minor dependence on x_0.

Since WIV has its origin in the wake developed in the gap between the cylinders, it is expected that the centre-to-centre separation between a tandem pair has a major effect on the response of the downstream body. In Assi *et al.* (2010) we have suggested that as x_0/D is increased the fluid force induced by upstream vortices is reduced due to diffusion of vorticity and increasing flow three-dimensionality. This theory is supported by the results presented in figure 4 showing that the response curve has indeed a strong dependence on x_0. Our results are in good qualitative agreement with those of Laneville & Brika (1999) even though they have performed tests with flexible tubes.

Figure 4(*b*) shows the dominant frequency of oscillation for each case plotted above. At first sight it is remarkable that all data points collapse over the range of separations investigated. During the beginning of the VIV regime the frequency curve follows closely the $St = 0.2$ line until $f = f_0$, but later it departs from this line to follow the lock-in behaviour observed for a single cylinder within the synchronization regime. But where the typical VIV regime would have finished for a single cylinder, say for $U/Df_0 > 15$, the f/f_0 curve remains on the same trend as before, which is distinctively lower than $St = 0.2$. Even for larger separations of $x_0/D = 20$, in which the response resembles that of simple VIV, the dominant frequency is observed not to return to $St = 0.2$ after the end of the supposed synchronization, but instead it remains at a much lower level for the rest of the reduced velocity range with $\hat{y}/D$ around 0.2.

This is the first evidence that there must be a fluid force with a lower frequency that sustains the response – a frequency that is lower than the vortex shedding frequency of both cylinders. The frequency of this fluid force appears not to vary with x_0 and shows only a small dependence on reduced velocity or Reynolds number when compared to the $St = 0.2$ line, for example.

3.1. *WIV response of the downstream cylinder at* $x_0/D = 4.0$

In order to investigate the mechanism behind WIV we will now concentrate our attention on a single separation; later we shall return to the effect of x_0/D on the response. A separation of $x_0/D = 4.0$ was chosen for various reasons: (i) it was beyond the critical separation where a bistable reattachment of the shear layers may occur, therefore a developed wake was observed to be present in the gap for all flow speeds; (ii) it gave a WIV response that is qualitatively consistent with other larger separations, being the most energetic behaviour observed; (iii) the cylinder displacement and magnitude of fluid forces were rather large and provided accurate measurements with the load cell; (iv) and the separation was not too large to fit in the particle image velocimetry (PIV) field of view.

Figure 5 presents the WIV response of the downstream cylinder of a pair, initially in tandem, with $x_0/D = 4.0$. The same pair of springs was employed during the whole experiment and the velocity of the flow in the test section was varied in order to cover a large range of reduced velocity, therefore yielding $Re = 2000$–$25\,000$. Figure 5(*a*) plots displacement versus reduced velocity with $\hat{y}/D$ being the harmonic amplitude of displacement. Although it gives a good idea of the average amplitude of vibration for many cycles of oscillation, $\hat{y}/D$ does not offer a good estimation of the maximum amplitude the cylinder might reach if displacement is varying from cycle to cycle. By actually counting individual peaks of oscillation it was possible to estimate a maximum and a minimum peak amplitude taking an average of the 10 % highest and 10 % lowest peaks of the whole series, yielding $[\hat{y}/D]_{max}$ and $[\hat{y}/D]_{min}$ respectively. Therefore we can say that for a certain reduced velocity the cylinder oscillates on average with $\hat{y}/D$ but reaches the maximum and minimum limits given

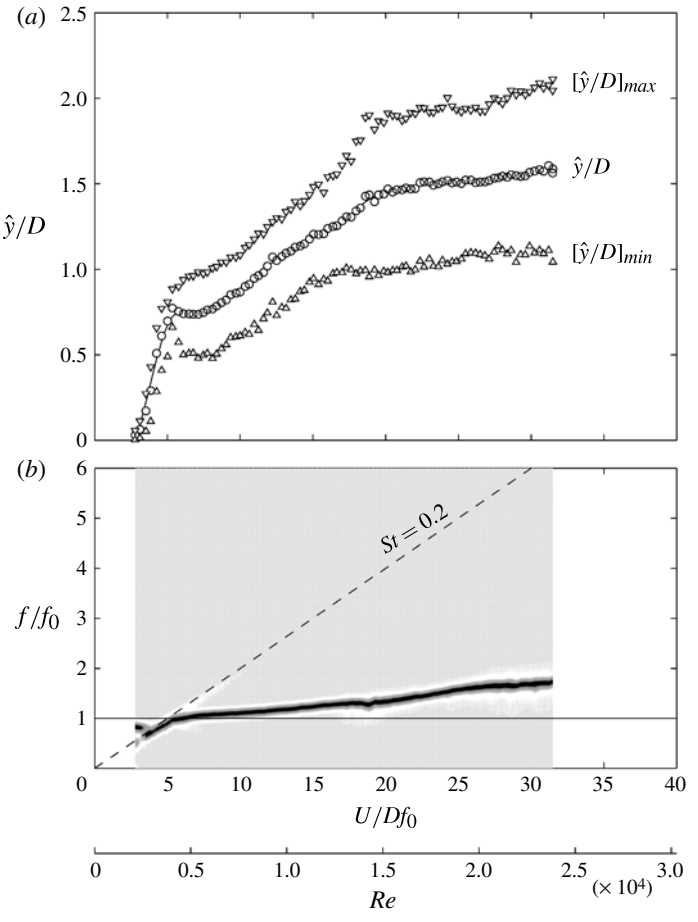

FIGURE 5. WIV response of the downstream cylinder at $x_0/D = 4.0$: (*a*) average displacement and average of maximum and minimum peaks; (*b*) normalized PSD of frequency of oscillation.

by the other two curves. This brings considerable new information about the response since it shows that $\hat{y}/D$ is not only building up with reduced velocity, but also the deviation from the average amplitude is increasing, i.e. the width of the envelope is also increasing.

Figure 5(*b*) shows the frequency of oscillation versus reduced velocity, the same data presented for $x_0/D = 4.0$ in figure 4 but now plotted as normalized PSD. It shows that f indeed follows a branch with values greater than f_0 but still not related to $St = 0.2$. However, the PSD contours also reveal that any other secondary frequency or harmonic present in the spectrum of oscillation is much smaller than the single dominant branch that is evident across the reduced velocity range. That is to say that there is no significant trace of a frequency branch associated with $St = 0.2$ beyond reduced velocity 10, with only a hint appearing between 5 and 10 (represented by white shading around the dashed line).

In Assi *et al.* (2010) we discussed in detail the behaviour of the lift force acting on both cylinders. For now it is enough to remember that the upstream cylinder

is shedding vortices as a single static body with $St \approx 0.2$. This was evident from measurements of lift as well as velocity fluctuation in the wake of the upstream cylinder. On the other hand, the lift force on the downstream cylinder has shown two clear branches bifurcating from the VIV resonance point (refer to figure 10 in Assi *et al.* 2010). The lowest branch corresponds to the frequency of oscillation in figure 5, but the highest branch is clearly associated with a vortex shedding frequency that follows the $St = 0.2$ line. This frequency may originate in the vortex shedding mechanism occurring on the upstream cylinder, or on the downstream cylinder, or on both.

Looking again at the response curve in figure 5 it is quite apparent that three different regimes can be identified and related to different inclinations of the displacement curve: (i) a VIV resonance hump (upper branch) around $U/Df_0 = 5$; (ii) a combined VIV (lower branch) and WIV regime roughly in the range $U/Df_0 = 5$–17; and (iii) a WIV regime for $U/Df_0 > 17$.

We conclude that the WIV response of the downstream cylinder of a pair is distinctively different from the VIV response of a single cylinder. Although some aspects are common to both types of FIV, especially those related to the overlap of VIV regime in the WIV response, others are very different. So far, it is clear that the low frequency of response observed for high reduced velocities is not directly associated with the vortex shedding mechanism of either cylinder.

4. Results: steady fluid forces on static cylinders

Traditionally, quasi-steady theory has been employed in an attempt to model various fluid-elastic phenomena. Therefore, we have also performed experiments with a pair of static cylinders in order to evaluate the behaviour of fluid forces acting on the downstream body in various staggered arrangements. Measurements were obtained by holding the upstream cylinder fixed and traversing the downstream cylinder across 160 stations (each marked by a small cross in figure 6) in and out of the wake interference region at $Re = 19\,200$.

Figure 6(*a*) presents the map of steady lift (or mean lift) acting on the downstream cylinder for different regions of wake interference. A negative value of $\overline{C}_y$ indicates lift force acting towards the centreline. As expected, the first evident observation is that the steady lift force points in the direction of the centreline for all configurations investigated. The $\overline{C}_y$ map reveals two regions of intense steady lift as high as -0.8. The first region between $x_0/D = 1.5$–2.5 is associated with the gap-flow-switching mechanism (described in Zdravkovich 1977) occurring in the first wake-interference regime, i.e. when fully developed vortices do not form in the gap. The second region with intense lift occurs for larger lateral separations around $y_0/D = 0.8$. Beginning around $x_0/D = 2.5$–3.0 with $\overline{C}_y \approx -0.8$, it develops into a trend of maximum $\overline{C}_y$ (indicated by the dash-dotted line) that decreases in intensity as the second cylinder moves farther downstream. For $x_0/D > 3.0$, it is observed that the magnitude of $\overline{C}_y$ continually decreases on increasing the separation, but the transverse extent of the force field increases farther downstream as the wake widens. This second region is associated with the second interference regime in which the upstream shear layers are not able to reattach to the downstream cylinder but roll up to form a developed vortex wake in the gap, i.e. what we are calling WIV.

In the steady drag map presented in figure 6(*b*) positive contours of $\overline{C}_x$ denote drag in the streamwise direction. Dotted lines represent contours of zero or negative drag that occur when the cylinders are close enough for the gap flow to be enclosed

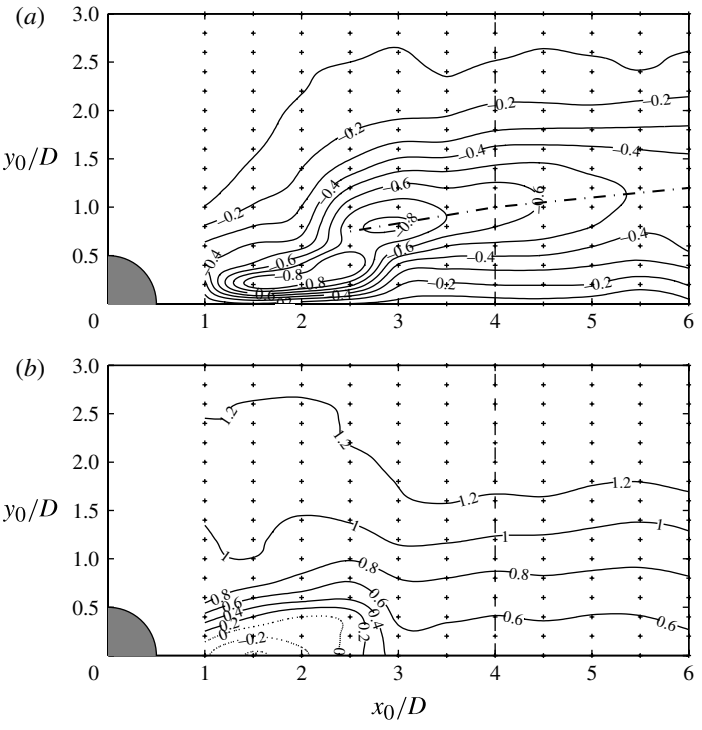

FIGURE 6. Contours of (*a*) steady lift ($\overline{C}_y$) and (*b*) steady drag ($\overline{C}_x$) on the downstream cylinder of a static pair. $Re = 19\,200$.

by the reattaching shear layers. For $x_0/D > 2.5$ the downstream cylinder in tandem arrangement only experiences positive drag indicating that a developed wake can now be formed in the gap. This critical separation coincides with the overlap of the two trends of maximum $\overline{C}_y$ presented in figure 6(*a*). While the downstream cylinder is immersed in the wake of the upstream cylinder the steady drag will be lower than that expected for a single cylinder exposed to a free stream. Only for lateral separations greater than $y_0/D = 1.5$ does this shielding effect disappear and $\overline{C}_x$ reaches values above 1.0. Our experimental results for the steady components are in very good agreement with other works found in the literature, including the maps produced by Zdravkovich (1977) and Bokaian & Geoola (1984).

4.1. *Detailed map for* $x_0/D = 4.0$

Since we are concentrating our attention on $x_0/D = 4.0$ we present a more detailed investigation of the steady fluid forces acting on the downstream cylinder for this separation. These results will be the basis for the discussion that will follow.

Starting from the $\overline{C}_y$ and $\overline{C}_x$ maps above, we can keep the downstream cylinder at $x_0/D = 4.0$ and traverse it in small steps across the wake along the vertical dashed line plotted in figure 6. If we now vary *Re* for each one of these stations we have the detailed curves presented in figure 7. Once more, it shows that the steady lift acting on the downstream cylinder points towards the centreline of the wake for all y_0/D separations. An almost linear behaviour is observed for the range $-1.0 < y_0/D < 1.0$ with a maximum of absolute $\overline{C}_y = 0.65$ found just past $y_0/D = -1.0$. Beyond that

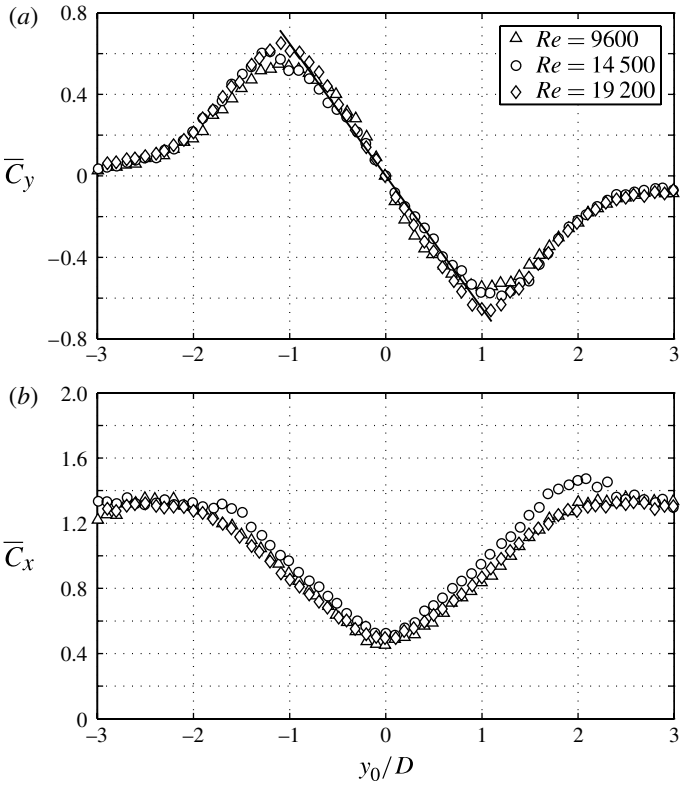

FIGURE 7. Steady fluid forces on a static downstream cylinder at $x_0/D = 4.0$ and various staggered positions.

separation the steady lift gradually reduces until it is beyond the influence of the wake and reaches zero around $y_0/D = 3.0$.

In figure 7(*b*) the steady drag curve reveals the shielding effect of the wake by showing an almost 60 % reduction in drag at the centreline; however the mean drag never attains negative values (drag inversion) for this separation. Bokaian & Geoola (1984) observed that the distribution of the drag coefficient is insensitive to a limited increase of *Re* from 2600 to 5900. Price (1975) also observed the same independence from *Re* for a range one order of magnitude higher. We also conclude that the steady fluid forces, lift and drag, do not vary with *Re* for the range of the experiments ($Re = 2000$–$25\,000$). In fact, several *Re* within this range were analysed but only three are plotted in figure 7 for clarity. This explains why our maps from figure 6 for $Re = 1.9 \times 10^4$ are in good agreement with Zdravkovich's (1977) for $Re = 6 \times 10^4$.

5. Experiment without springs: $f_0 = 0$

In Assi *et al.* (2010) we performed an idealized experiment by removing the unsteadiness of the upstream wake generated by vortices being shed from the upstream cylinder. In that case we made $f_s = 0$ and concluded that a cylinder immersed in such a steady wake would not develop WIV. We were convinced that the interaction between the oscillating cylinder and the unsteady wake from upstream is crucial to sustain the WIV mechanism. The necessary phase lag that drives and maintains the

excitation was shown to originate in this complex vortex–structure interaction. But one question was still left unanswered: Why is the cylinder oscillating at a frequency that is distinctively different from both the upstream vortex shedding frequency (f_s) and the natural frequency of the system (f_0)? WIV turned out to be understood as a non-resonant mechanism with the amplitude of response increasing far beyond any synchronization range. The fact that the excitation mechanism is not dependent on the forcing frequency matching f_0 gave us the idea of removing yet another fundamental frequency of the system. In the previous experiment we made $f_s = 0$ by generating a steady shear profile without vortices; now we make $f_0 = 0$ by removing the springs of the oscillator.

The same experimental set-up was employed. While mass (m) and damping (c) remained unchanged, the pair of springs was removed from the system so that $k = 0$ and $f_0 = 0$. Therefore, for the downstream cylinder immersed in still water there was no structural stabilizing force whatsoever to keep it in position. Cylinders were initially aligned in tandem, but the downstream body would drift away from the centreline, responding to any perturbation coming from the flow or from the rig.

We found no other works on WIV of cylinders where all stiffness had been removed. Zdravkovich (1974) performed experiments with a downstream cylinder mounted on a horizontal swinging arm without springs, but he was left with a restoration force generated by the steady flow. The drag acting on the cylinder generated a stabilizing force component towards the centreline – in the same way that the weight stabilizes a vertical pendulum in free oscillation – resulting in an equivalent stiffness generated by the flow. Most of his experiments were concerned with the gap-flow-switching mechanism, hence were concentrated in the proximity interference region. For $x_0/D < 3.5$ he observed severe vibrations with a clear dominant frequency; yet the response was abruptly reduced for separations between $x_0/D = 3.5$–7.0 with no clear dominant frequency being identified. Beyond that critical separation the downstream cylinder was not prone to gap flow switching any longer but on entering the WIV region still the expected build-up of response was not observed. Zdravkovich's experiment was performed in air and his elastic rig presented a very high damping factor of $\zeta = 0.24$. Probably, we believe, a high value of combined $m^*\zeta$ was enough to suppress WIV but not gap flow switching, only proving that the content of energy in the first mechanism is lower than in the latter. Apart from this experiment we have not seen any other WIV investigation on cylinders mounted without springs – and even in this case there was still a remaining stabilizing force left due to resolved drag.

5.1. *WIV response without springs*

In the WIV response with springs we found that a VIV resonance peak always occurred around $U/Df_0 = 5.0$, before a pure WIV mechanism could prevail. A hypothesis is that the cylinder was being excited by VIV up to a condition of motion (coupled displacement and frequency) from which WIV could eventually take over. But now, once the springs are removed, we do not expect to see the local peak of VIV appearing, consequently the cylinder may not be excited into the critical motion for WIV to start. Would it still be possible to obtain a WIV response without first passing through a VIV resonance peak?

We already know that a static downstream cylinder in a staggered arrangement experiences a steady lift force towards the centreline. Keeping this stabilizing effect in mind, we expect that a free downstream cylinder mounted without springs would respond in one of the three possible ways.

(i) *Drift sideways:* the impulse generated by the vortex–structure interaction would be strong enough to overcome $\overline{C}_y$ towards the centreline; the cylinder would drift away beyond the wake-interference region (static divergence) and no oscillatory motion would be sustained.

(ii) *Remain stable on the centreline:* the impulse generated by the vortex–structure interaction when the cylinder is on the centreline would be too weak to displace the cylinder and initiate any WIV; the cylinder would find a stable position on the centreline due to a strong $\overline{C}_y$ field and no oscillatory motion would be sustained.

(iii) *Develop oscillatory motion:* the impulse generated by the vortex–structure interaction would be strong enough to displace the cylinder, but the stabilizing $\overline{C}_y$ would restore the cylinder towards the centreline. A phase lag between force and displacement would appear to build up the WIV mechanism and sustain oscillatory motion even without springs.

In principle it appears that the existence of oscillatory motion depends on the balance between the impulse force from the vortex–structure interaction and the stabilizing lift towards the centreline, at least in a system without springs. But since both force components depend on the unsteady wake configuration and motion of the body we cannot predict *a priori* if the system will respond with sustainable oscillatory motion – and even if some oscillation is developed there is no indication that it would resemble the WIV response obtained when springs were present.

Figure 8 presents the WIV response for the downstream cylinder mounted without springs compared with the curve already presented for a cylinder with springs. Both curves were obtained for the same variation of the flow speed; therefore both data sets share the same Reynolds number scale. But because the system without springs has no inherent f_0 it does not make sense to plot this curve with a reduced velocity axis. In fact, by making $f_0 = 0$ we are effectively making $U/Df_0 = \infty$ for all points of the response without springs; the variation of flow speed can only be represented by Re in this case.

From among the three hypotheses presented above, the response certainly agrees with the third one concerned with sustainable oscillatory motion. Not only was the cylinder able to sustain oscillations, but most surprisingly the amplitude of response was remarkably similar to the case with springs. As far as the amplitude of response is concerned, it appears that the absence of springs is insignificant for the WIV mechanism. As expected, the local peak of VIV around $U/Df_0 = 5.0$ disappeared once the resonance $f_s = f_0$ was eliminated by removing the springs. However, the overall response for both cases, with and without springs, is notably similar. The fact that $\hat{y}/D$ increases with flow speed is not an effect of reduced velocity; in other words, the increase in WIV response observed for a cylinder without springs cannot be related to any structural stiffness. Instead, it seems that the response reveals some dependence simply on Reynolds number. Since both curves are essentially very similar, we suggest that an independence of response from reduced velocity and a dependence on Re might also be occurring for the cylinder mounted with springs. We shall return to this subject later on.

Let us turn now to the frequency of response presented in figure 8(*b*). Since f_0 is not defined for the case without springs, we can only compare both curves if they are plotted in dimensional form (s^{-1}). The response with springs was analysed above, but it is convenient to summarize it here once more: f follows the $St = 0.2$ line up to the VIV resonance; then follows close to f_0 through a distorted synchronization range, but eventually continues on a distinct branch dominated by pure WIV. On the other hand, the frequency of response without springs shows no effect of VIV synchronization

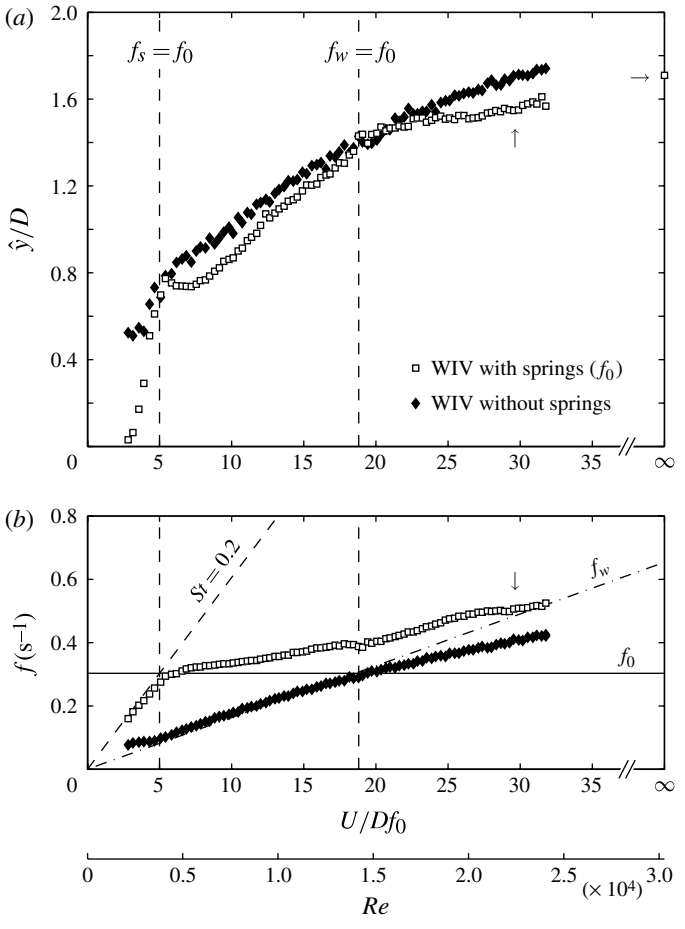

FIGURE 8. WIV response of a downstream cylinder mounted with and without springs at $x_0/D = 4.0$: (*a*) displacement; (*b*) dominant frequency of oscillation.

– that is obvious since there is no f_0 for it to be synchronized with – but follows an almost straight line as the flow speed is increased. In fact, we note that it follows very closely the dash-dotted line marked as f_w, which shall be explained later. Another way to analyse this result is to create a non-dimensional parameter fD/U, a type of Strouhal number, plotted in figure 9. This way, the $St = 0.2$ line presented in figure 8 becomes a constant in figure 9 and all the data are distorted to incorporate the effect of U varying in both axes. We shall return to this graph after some analytical modelling that will follow in the next sections. Before that, we will look at the time series of displacement and lift.

Figure 10 shows three examples of time series for the WIV response without springs. The flow speed in each case, represented by Re, would correspond to a reduced velocity of $U/Df_0 = 10$, 20 and 30 for the cylinder mounted with springs (which can be compared with the plots in Assi *et al.* 2010). The displacement plots on the left (*a,c,e*) show that the system is indeed responding with oscillatory motion. Although the frequency of response seems to be rather regular, it is evident that the envelope of amplitude varies from cycle to cycle throughout the series.

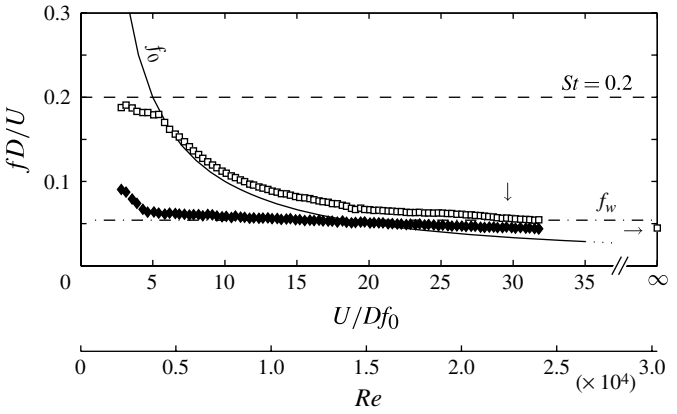

FIGURE 9. Non-dimensionalized dominant frequency of oscillation of a downstream cylinder mounted with and without springs. See figure 8 for key.

Figure 10(*b,d,f*) presents superimposed plots of displacement and lift for similar cycles around the average value of $\hat{y}/D$ given in figure 8.

A considerable variation in displacement is evident from the deviation of dark-grey lines from the average cycle represented in black. Nevertheless, it is the irregularity of the lift force that really catches the attention. A clutter of light-grey lines reveals that almost no cycle is identical to any other and an abundance of higher frequencies induce C_y to present significant fluctuations within a single cycle of displacement. Once more we can note that intense, high-frequency fluctuations in lift, a consequence of the instantaneous interaction between cylinder and wake, may have a similar effect as generating the phase lag between y and C_y that is necessary to transfer energy from the flow to the structure. However, by looking at the average cycle of lift, given by a dashed-black line, we can still note a lower frequency component almost, but not exactly, out of phase with the displacement. This term must have some inertia component reacting against the acceleration of the body; part must be related to the flow excitation, but part must also be related to the steady $\overline{C}_y$ field acting towards the centreline.

Analysing the PSD of C_y of both cylinders (figure 11) we note that the upstream cylinder (figure 11*a*) is shedding vortices as an isolated body, with no interference from the motion of the second cylinder propagating upstream. This was also observed for the case with springs and there is no reason to expect that it would be different for the same separation. On the other hand, the PSD of lift on the downstream cylinder shows two distinct branches of frequency: the higher $f(C_y)$ branch is clearly an effect of vortex shedding from the upstream cylinder; whereas the lower $f(C_y)$ branch is promptly identified with that frequency of response observed in figure 8. It is important to note that in this case there is no f_0 defined by springs (that is why $f(C_y)$ has a dimension of s^{-1}), hence the fact that $f(C_y)$ presents a lower branch is not associated with any structural stiffness. It is only at the very beginning of the scale, for $Re < 0.3 \times 10^4$, that we see the vortex shedding branch having more energy than the lower one; otherwise, for the rest of the response curve, the lower frequency branch clearly dominates the character of C_y. Now, with such a clear preponderance of the lower $f(C_y)$ branch it is not surprising that the dominant frequency of response matches this major excitation.

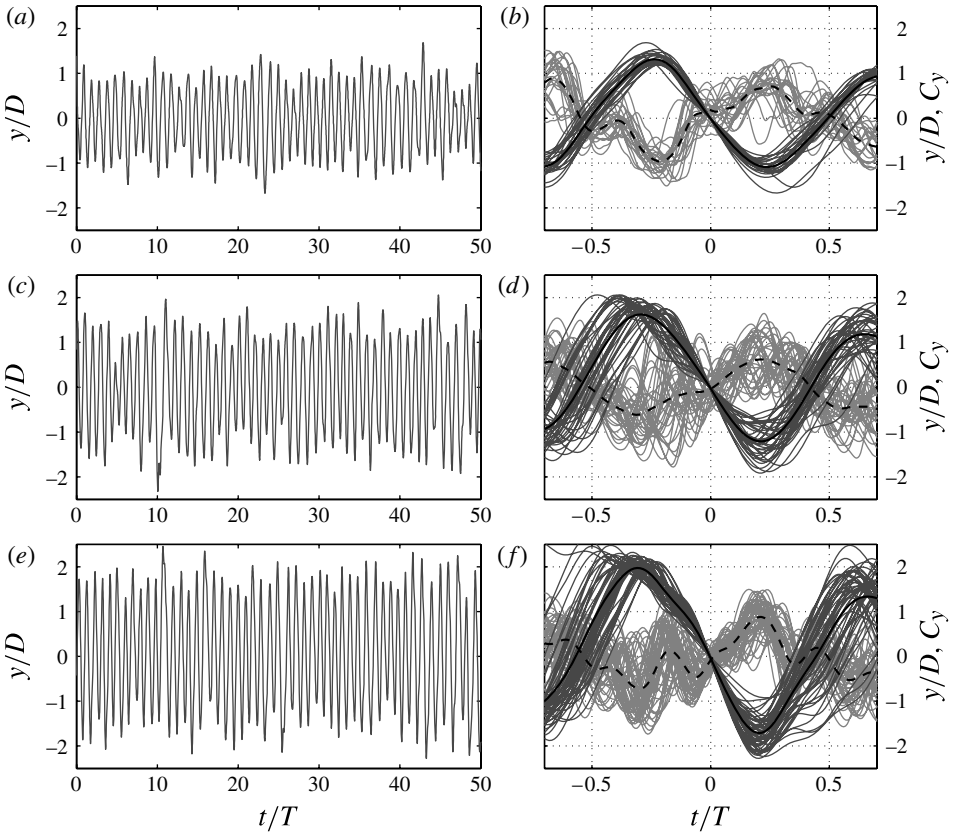

FIGURE 10. Three examples of time series for WIV without springs. (*a,c,e*) Displacement signal for around 50 cycles of oscillation. (*b,d,f*) Superimposed plots of similar cycles: y/D in dark grey and C_y in light grey with average cycle in black. (*a,b*) $Re = 0.8 \times 10^4$, (*c,d*) $Re = 1.5 \times 10^4$, (*e,f*) $Re = 2.3 \times 10^4$.

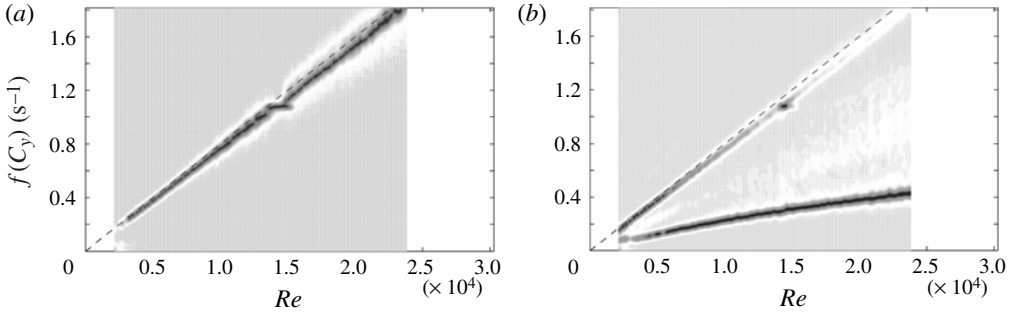

FIGURE 11. Normalized PSD of lift force acting on the (*a*) upstream static cylinder and (*b*) downstream cylinder without springs.

The body is able to sustain oscillatory motion even without any springs to create structural stiffness and we are still left with the question about the origin of a lower

frequency force that is not related to either f_s or f_0. The only possibility left is that there must be another force acting to restore the body to equilibrium. Since the body is essentially without any structural stiffness, such a stabilizing force has to be coming from the flow itself. That is to say that there must be a fluid force playing the role of the stiffness in the oscillator, otherwise no oscillatory motion would be observed. So we turn our attention once more to the steady lift generated in staggered arrangements.

6. The wake-stiffness concept

Now that we have observed that the WIV response without springs indeed presented oscillatory motion – with amplitude increasing with Reynolds number and a frequency distinct from f_s or any f_0 – we should model the problem of a cylinder with no structural stiffness. The equation of motion (1.1) has the stiffness term removed if we make $k = 0$ for a downstream cylinder without springs, resulting in

$$m\ddot{y} + c\dot{y} = C_y \tfrac{1}{2}\rho U^2 D, \tag{6.1}$$

where all forces are per unit length of cylinder.

Applying the same 'harmonic forcing and harmonic motion' assumption, where $y = \hat{y}\sin(2\pi ft)$ and $C_y = \hat{C}_y \sin(2\pi ft + \phi)$, results in

$$\frac{\hat{y}}{D} = \frac{1}{4\pi}\hat{C}_y \sin\phi \frac{\rho U^2}{cf}. \tag{6.2}$$

Notice that neither the mass nor any stiffness comes into the equation, but the excitation is simply balancing the structural damping of the system given by c (friction damping per unit length of cylinder). Rearranging (6.2) into non-dimensional groups results in

$$\frac{\hat{y}}{D} = \frac{1}{4\pi}\hat{C}_y \sin\phi \left(\frac{U}{Df}\right)\left(\frac{\rho UD}{\mu}\right)\left(\frac{\mu}{c}\right). \tag{6.3}$$

Knowing that the dynamic viscosity μ is a physical property of the fluid and assuming that viscous damping per unit length c is only based on the friction of the air bearings, we conclude that μ/c does not vary with Reynolds number. We are left with three non-dimensional groups: (i) $C_y \sin\phi$ is associated with the excitation force, we call it the vortex-impulse term and will consider it later; (ii) U/Df represents the inverse of a non-dimensional frequency of oscillation; (iii) $\rho UD/\mu$ is the Reynolds number.

6.1. *Frequency of oscillation and natural frequency of wake stiffness*

Let us first investigate the behaviour of the non-dimensional oscillation frequency (fD/U). If we consider the map of steady lift across the wake for $x_0/D = 4.0$ presented in figure 7 we note that $\overline{C}_y$ acting towards the centreline has a rather good linear behaviour between $-1.0 \leqslant y_0/D \leqslant 1.0$ and does not vary within the *Re* range. Of course nonlinearities appear for larger separations, but we can estimate the slope

$$\left|\frac{\partial \overline{C}_y}{\partial(y_0/D)}\right| \equiv \Delta_{\overline{C}_y} \approx 0.65 \tag{6.4}$$

with 95 % confidence inside the wake interference region (considered to be $-1.0 \leqslant y_0/D \leqslant 1.0$ in this analysis). For convenience, we shall refer to this slope simply as $\Delta_{\overline{C}_y}$ from now on.

We know that this steady lift works as a restoring force towards the centreline. Similarly to the stiffness generated by a spring, the magnitude of $\overline{C}_y$ increases linearly with transverse displacement of the cylinder, at least within the wake interference region. For that reason, the $\overline{C}_y$ field can be understood as a 'fluid-dynamic spring' generated by the flow; such an effect will be referred to as *wake stiffness* from now on.

The equivalent spring constant per unit length (k_w) that would generate such a flow effect is

$$k_w = \Delta_{\overline{C}_y} \tfrac{1}{2}\rho U^2; \tag{6.5}$$

thus an equivalent natural frequency f_w could also be associated with the wake stiffness as

$$f_w = \frac{1}{2\pi}\sqrt{\frac{k_w}{(m^* + C_a)\rho\dfrac{\pi D^2}{4}}}, \tag{6.6}$$

where C_a denotes the potential added mass coefficient to take into account the effect of the added inertia of the displaced water.

Since wake stiffness is a fluid-dynamic force, its effect would be equivalent to a spring with a k_w that increases with U^2, as seen in (6.5); hence the associated natural frequency f_w increases linearly with Re. Replacing (6.5) in (6.6) and multiplying it by D/U results in a Strouhal-type non-dimensional parameter

$$\frac{f_w D}{U} = \frac{1}{2\pi}\sqrt{\frac{2}{\pi}\frac{\Delta_{\overline{C}_y}}{(m^* + C_a)}}. \tag{6.7}$$

We already know that $\Delta_{\overline{C}_y}$ is invariant with Re. Since C_a cannot vary with Re either, we conclude that $f_w D/U$ is a constant irrespective of Re.

Turning back to figure 8 we note that the frequency of oscillation f for a cylinder without springs presents a remarkable linear behaviour that grows with Re, which is represented by an almost constant curve far from $St = 0.2$ in figure 9. This suggests that there must be a preferred frequency lower than f_s dominating the response. Note that this characteristic frequency cannot be related to f_0 because the system has no springs. Therefore we are left with the possibility that this restoration is indeed coming from the $\overline{C}_y$ field, hence it must be related to $\Delta_{\overline{C}_y}$.

Now if we substitute the numerical values $\Delta_{\overline{C}_y} = 0.65$, $m^* = 2.6$ and $C_a = 1.0$ in (6.7) we find that $f_w D/U = 0.054$, which is represented by the f_w dot-dashed line in figures 8 and 9. The agreement between f_w and the WIV response without springs is remarkable. This is evidence that a cylinder without springs may also be responding to the wake stiffness with $f = f_w$ for the whole range of Re. That is to say that the excitation frequency identified in the lower branch of $f(C_y)$ in figure 11 – the one that matches the response frequency f in figure 8 – is actually governed by the wake stiffness effect described in (6.5) to (6.7).

If it is true that $f = f_w$, (6.7) tells us that fD/U is also a constant and the cylinder indeed oscillates with f that increases linearly with Re. In figure 8 we note that f closely follows f_w up to around $Re = 1.5 \times 10^4$ when the response amplitude reaches about $\hat{y}/D = 1.4$. Beyond this point the amplitude grows towards values around $\hat{y}/D = 1.8$ meaning that the cylinder is oscillating further out of the wake interference region. From the $\overline{C}_y$ map for $x_0/D = 4.0$ (figure 7) we know that the

steady lift grows linearly with lateral separation up to around $y_0/D = 1.0$. Beyond that, nonlinear effects start to appear and the wake stiffness is not able to be represented simply by the slope $\Delta_{\overline{C}_y}$ but would gradually be reduced. This is exactly what is observed as the frequency curve begins to depart from the f_w line as $\hat{y}/D$ increases. Of course some effect in reducing f must be coming from the fact that secondary effects in the effective added mass of fluid may appear as the cylinder moves in and out of the wake interference region. But even considering that the effective added mass is constant throughout *Re* the agreement is still very good.

Although it is very helpful to think of the wake stiffness effect as a linear spring, a quasi-static lift map still is an oversimplification of the problem. If the restoring fluid force towards the centreline is induced by complex vortex–structure interactions – as proposed in Assi *et al.* (2010) – it should also present unsteady variations as the cylinder moves across the wake. However, we can still imagine that if the cylinder is displaced farther away from the wake interference region ($y/D \gg 1.0$) the induced force at that instant must be reduced. On the other hand, if in another instant the cylinder is located closer to the wake boundary the vortex-induced force can be amplified. For that reason we could suggest that the total excitation force must be composed of two fluctuating terms with distinct frequencies: one term is associated with the wake stiffness, which obviously depends on the position of the body across the wake and is related to f; the other is associated with the impulse vortex-force induced on the cylinder, which also depends on the lateral position of the cylinder and is thus related to f_s. We believe that while a series of vortices streaming along the wake induces a steady force towards the centreline, each vortex also induces an instantaneous force fluctuation (an impulse) on the cylinder. The magnitude of both *wake-stiffness* and *vortex-impulse* terms will depend on the relative position of the body and a particular interaction with the wake.

6.2. *VIV and WIV resonances:* $f_s = f_0$ *and* $f_w = f_0$

If the wake-stiffness is dominant over the vortex-impulse term it is straightforward to predict that the cylinder should respond with $f = f_w$ and not $f = f_s$. As we have seen so far $f_w D/U$ does not vary with flow speed, thus f_w increases linearly with *Re*. Since f_0 is a constant defined by the springs, there must be a critical point where the wake stiffness has the same intensity as the spring stiffness, i.e. $k_w = k$ and $f_w = f_0$. This occurs in figures 8 and 9 where f_w crosses the f_0 line at $Re = 1.2 \times 10^4$ (equivalent to $U/Df_0 = 18.8$ for the case with springs). We know the present set of coil springs provides the system with a measured stiffness of $k = 11.8$ N m^{-1}. But considering the steady lift map with $\Delta_{\overline{C}_y} = 0.65$ in (6.5) we see that the wake stiffness can reach values as high as $k_w = 34$ N m^{-1} at the end of the *Re* range of the experiments.

For the case with springs we find f following closer to the f_0 line during the range where VIV is relevant, with the lock-in peak occurring around the intersection of f with both f_0 and $St = 0.2$ lines. This first VIV resonance is marked by the vertical line $f_s = f_0$ in figure 8. At this point $k_w = 1.8$ N m^{-1} is only 15 % of k provided by the springs. As the flow speed is increased the VIV synchronization tends to disappear as $St = 0.2$ moves away from f_0. At the same time the wake stiffness is also getting stronger until both k_w and k have the same value. As we saw, this occurs for $U/Df_0 = 18.8$ and is marked by the second WIV resonance line $f_w = f_0$, beyond which k_w is greater than k.

The two resonance lines divide the response for a cylinder with springs into three regimes that are best identified in figure 8. (i) Before $f_s = f_0$, when $St = 0.2$ is

approaching f_0, the displacement resemble an initial branch of VIV and f follows the Strouhal line up to the resonance peak. (ii) The second regime, between $f_s = f_0$ and $f_w = f_0$, is marked by a steep slope in the displacement curve; f remains rather close to f_0 as the VIV synchronization range gradually gives way to a wake stiffness that is growing stronger with Re. (iii) The third regime, beyond the second resonance $f_w = f_0$ is characterized by a change of slope in both the displacement and frequency curves. With $k_w > k$ the WIV response is established and dominates alone for the rest of the Re range.

The system works as if the set of springs were important only in the first regime before the $f_w = f_0$ resonance, but the system completely overlooks its small structural stiffness given by f_0 as k_w gets relatively stronger. It appears that away from the resonances $f_s = f_0$ and $f_w = f_0$ the spring acts against the WIV excitation with the effect of reducing the amplitude of vibration. This idea is in agreement with the classical theory of linear oscillators; if the excitation force is outside the resonance of the system the response will not be as high as the resonance peak.

Various experiments have investigated the flux of energy in the system for a cylinder oscillating in forced vibrations in a flow. Recently, Morse & Williamson (2009) have presented a detailed energy map for VIV of a single cylinder. If we take values of displacement and frequency from our own WIV curves and plot them in their VIV energy map we will see that the structure is actually losing energy to the flow. If we assume that the major forcing term is coming from the WIV mechanism governed by wake stiffness, the VIV part governed by spring stiffness is contributing to dissipate energy and reduce the vibration. That is why the response curve with springs shows reduced amplitude away from the two resonance lines when compared with the case without springs. Because our excitation force is believed to have a wake-stiffness and a vortex-impulse component, each related to one characteristic frequency, the response will be slightly accentuated when $f_s = f_0$ (VIV resonance) and $f_w = f_0$ (WIV resonance).

One could ask if it would be possible to have a third resonance $f_s = f_w$, potentially occurring also for a cylinder without springs. Since both $St = 0.2$ and f_w are dependent on Reynolds number, they would have to be equal throughout the whole Re range. Starting from (6.7) and considering that the Strouhal number of a cylinder is roughly constant with Re, there are only two ways to bring both $St = 0.2$ and f_w lines together.

Firstly, fixing the mass of the system we would have to generate a steady lift field with $\Delta_{\overline{C}_y} = 8.9$ which is one order of magnitude higher than the maximum value measured for staggered cylinders. Now, if the steady lift towards the centreline has its origin in the unsteady vortex–structure interaction, both f_s and f_w originate in the same phenomenon and have to coexist within physical boundaries. By this we mean that the wake structure required to generate such an intense steady field would have to be very different from the vortex shedding mechanism that we know. Therefore we do not expect $f_s = f_w$ due to such an intense $\overline{C}_y$ field.

Secondly, knowing that $\Delta_{\overline{C}_y}$ is invariant with Re, we can change the mass of the system in order to change the natural frequency f_w. Keeping $\Delta_{\overline{C}_y} = 0.65$ and $C_a = 1.0$ constant in (6.7) and equating the right-hand side to $St = 0.2$ results in $m^* = -0.74$. Since this result is impossible in a physical system we can affirm that $St = 0.2$ and f_w will never overlap.

In fact, since we know the cylinder is responding to WIV with $f = f_w$, to have $f_w = f_s$ means that the cylinder would be oscillating at the frequency of vortex shedding for the whole Re range. This is the WIV equivalent of the phenomenon

described by Govardhan & Williamson (2002) for VIV of a single cylinder. They verified that for m^* below a critical value around 0.54 the VIV response would persist for an infinite regime as if the lower branch were extended indefinitely. It was observed that the frequency of oscillation f would follow the vortex shedding frequency f_s, linearly increasing with reduced velocity, sustaining a regime they called 'resonance forever'. Although this appears to be physically impossible in our case, we hypothesize that if we could artificially bring both $St = 0.2$ and f_w lines together – in a force feedback system this would be possible – the cylinder would vibrate indefinitely with both VIV and WIV perfectly combined.

6.3. *Response without springs in a shear flow*

In Assi *et al.* (2010) we have seen that the unsteadiness of the wake was necessary to excite WIV; a cylinder immersed in an artificial wake without vortices did not respond with WIV. In the present paper we investigated the importance of the wake-stiffness effect in sustaining the vibration of a cylinder mounted without springs. Finally, we can combine the two concepts of wake stiffness and vortex impulse in the response of a cylinder immersed in a shear flow (without unsteady vortices) but also without springs (without structural stiffness). This experiment was performed and the result was that no vibration was observed.

Although some small wake-stiffness effect was left in the shear flow after vortices were removed – $\Delta_{\overline{C}_y} \approx 0.2$ could be estimated from the steady lift field in Assi *et al.* (2010) – it was not strong enough to sustain oscillatory motion and the cylinder did not respond with vibrations. If our theory is correct, we need to bring the excitation term from the vortex–structure interaction acting together with the wake-stiffness effect in order to produce a WIV response. Removing the unsteadiness of the upstream wake we are essentially left without the WIV excitation term, therefore the response will be that of VIV. But, by removing both the unsteadiness of the wake and the springs at the same time we are left with no response at all.

7. Dependence on Reynolds number

Returning to (6.3), we can now analyse the behaviour of the non-dimensional parameter $\hat{C}_y \sin\phi$ (that we are calling the vortex–impulse term) with respect to Reynolds number. We already know that the cylinder is responding with $f = f_w$, a dominant frequency produced by the wake stiffness effect. In the harmonic assumption applied in (6.1) we consider that the fluid force is represented by only a single dominant frequency and phase angle. However, in figures 10 and 11 we clearly see that C_y in fact presents two significant frequencies: a lower branch associated with wake stiffness and a higher branch associated with vortex–impulse from the upstream wake.

Retaining the harmonic hypothesis we could split the actual effect of C_y into two parts. Because f_w is clearly dominant over f_s let us consider that the magnitude of $\hat{C}_y$ is only produced by the wake stiffness effect and has very little influence from vortex–impulse fluctuations. Consequently, the fluid force would have a dominant component $f = f_w$, with magnitude depending only on $\Delta_{\overline{C}_y}$ and acting out of phase with the displacement (again we are entering quasi-static territory, but at least now we are supported by having $U/Df_0 = \infty$). On the other hand, we need to account for the phase lag necessary to sustain the vibration. We have already proposed (Assi *et al.* 2010) that it is generated by the complex vortex–structure interaction as the body

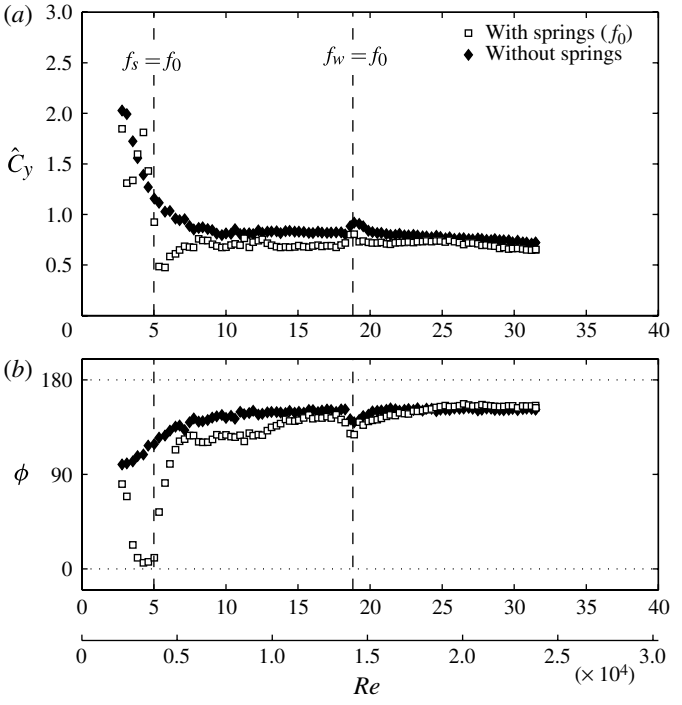

FIGURE 12. Comparison between lift coefficient (a) and phase angle (b) for the WIV response of a cylinder with and without springs at $x_0/D = 4.0$.

crosses the wake, therefore we could attribute the existence of ϕ to the vortex–impulse fluctuations operating at f_s.

We have shown that $\Delta_{\overline{C}_y}$ does not vary with Re, therefore $\hat{C}_y$ should also be invariant. However, we have also demonstrated that, due to fluctuations caused by vortex–impulse, the phase angle varies from cycle to cycle as the cylinder interacts with different wake configurations. Albeit not being very strong, this supposition finds some support in the time series presented in figure 10. Therefore, let us now investigate $\hat{C}_y$ and ϕ independently.

Figure 12(a) compares the total lift coefficient for WIV responses both with and without springs. An abrupt reduction in $\hat{C}_y$ for the case with springs is characteristic of the VIV phase shift and occurs at the $f_s = f_0$ resonance. We can still note some differences between the cases while VIV is losing strength between the resonances, but yet it is beyond the resonance $f_w = f_0$ that WIV clearly dominates and both curves follow each other closely for the rest of the Re range. Apart from a small range of $Re < 0.5 \times 10^4$, $\hat{C}_y$ without springs shows a fairly constant behaviour with a small negative slope. Figure 12(b) compares average values of ϕ for WIV responses with and without springs. Each data point was obtained by employing the Hilbert transform to calculate instantaneous values of phase angles and then averaging ϕ for more than 500 cycles of oscillation (refer to Assi 2009 for more details). The curve shows that ϕ without springs presents a relatively constant value around 153° for $Re > 0.5 \times 10^4$.

Although both $\hat{C}_y$ and ϕ appear to be fairly invariant with Re, we cannot forget that values plotted in figure 12 are averaged for as many as 500 cycles of oscillations.

We have already seen in figure 10 how irregular C_y can be from cycle to cycle. Variations within the present Re range are also expected to occur due to the complex characteristic of the wake. For example, it is known that the vortex formation length presents a strong variation with Re (Norberg 1998; Assi *et al.* 2006); and the three-dimensionality of the wake may also present some Re dependence. Nevertheless, although $\hat{C}_y$ and ϕ cannot be confirmed as strictly constant we are able to conclude that, to a first approximation, the non-dimensional term $\hat{C}_y \sin\phi$ should be roughly invariant with Re, at least within the subcritical Re range of the experiments.

Turning back to (6.3), we can now verify that μ/c, U/Df and $\hat{C}_y \sin\phi$ are approximately invariant with Re, leaving only the Reynolds number term itself on the right-hand side of the equation. As a result it is evident from this analysis that $\hat{y}/D$ is linearly dependent on Re and the WIV response should increase with flow speed up to a critical amplitude. Once the cylinder starts to be displaced out of the wake interference region nonlinear effects become important, limiting the response to an asymptotic value. Secondary effects may be acting on U/Df and $\hat{C}_y \sin\phi$ conferring on the response the curved shape presented in figure 8. The analysis developed above is in good agreement with displacement curves presented for both cases (with and without springs). Therefore we conclude that the mechanism that is building up the amplitude of vibration in WIV is definitely not a consequence of reduced velocity but a direct effect of Reynolds number.

Picking a displacement point from the curve without springs at an arbitrary value of $Re = 2.3 \times 10^4$ (the location represented by a vertical arrow in figure 8) we are able to estimate the limiting value the response is asymptotically approaching as $U/Df_0 \to \infty$ for that specific Re. Of course this is the data point from the curve without springs immediately above the vertical arrow, but it can also be represented on the right-hand axis for $U/Df_0 = \infty$ (this will be useful later when comparing different x_0/D separations).

Such a strong Re dependence turned out to be a rather unexpected result. It took us some time to comprehend how a fluid-elastic system could show large variations over such a short Re range. However, if we consider that our system actually possesses a fluid-dynamic spring that increases stiffness with U^2, a seen in (6.5), we are left with the only conclusion that $\hat{y}/D$ must indeed vary with Re.

7.1. *Experiments with constant Re*

At this point one may recall the results from Hover & Triantafyllou (2001), presented in figure 2(*b*), who measured the WIV response of a cylinder at $x_0/D = 4.75$ and constant $Re = 3 \times 10^4$. They achieved this by varying the spring stiffness of a force-feedback system. In spite of operating at a fixed Reynolds number, they were able to measure a build-up of response that increased with reduced velocity. In principle, this seems to contradict our theory that the WIV response is not affected by reduced velocity.

Considering that their separation of $x_0/D = 4.75$ must provide a wake-stiffness effect in the order of $\Delta_{\overline{C}_y} \approx 0.55$ (based in our figure 6), we can estimate that the critical reduced velocity at which the wake stiffness equals the spring stiffness ($k_w = k$) is as high as $U/Df_0 = 21$ (based in our $\overline{C}_y$ map of figure 6, $C_a = 1.0$ and their value of $m^* = 3.0$). However, the maximum reduced velocity achieved in their experiment is only around 17. Hence the regime Hover & Triantafyllou (2001) observed was still between the resonances $f_s = f_0$ and $f_w = f_0$, a region where VIV still has some significance.

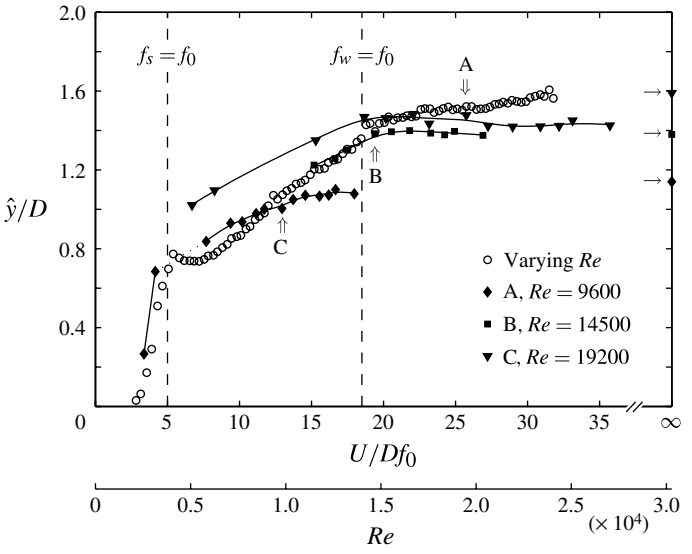

FIGURE 13. WIV response at constant Re for $x_0/D = 4.0$. Reduced velocity varied by changing the springs, compared to our reference cylinder with fixed springs and varying U/Df_0 by varying flow speed (the secondary axis of Re refers to this curve only).

According to our theory, we would expect their results to reach an asymptotic value around $\hat{y}/D = 1.5$ for $Re = 3 \times 10^4$, which is in good agreement with their curve reproduced in the present work (figure 2*b*). Note, however, that Hover & Triantafyllou (2001) do not plot $\hat{y}/D$ but an average of the 10 % highest peaks of displacement. As we have seen in figure 5 the maximum displacement of the cylinder can be considerably greater than the averaged $\hat{y}/D$ that we usually employ. The same observation is also true for the results obtained by Assi *et al.* (2006) also presented in figure 2(*b*). Even though k was constant, they could not reach the regime above the WIV resonance $f_w = f_0$ due to a limitation in the maximum flow speed.

In order to verify this phenomenon, we carried out a series of experiments for three constant Reynolds numbers at $x_0/D = 4.0$. The flow speed was fixed and reduced velocity was varied by changing the set of springs and, consequently, changing f_0. Figure 13 presents the results compared to our reference WIV response of a cylinder with fixed springs and varying U/Df_0 by varying flow speed (the secondary axis of Re refers to this curve only).

Three vertical arrows (A, B, C), one for each Re curve, mark the condition where the stiffness of the varying wake spring matches the fixed spring k. Hence all data points to the right of these arrows have a spring that is softer than our reference curve (and stiffer to the left). None of the curves was able to span the three regimes defined by the resonance lines $f_s = f_0$ and $f_w = f_0$, but considering the results of all three curves we are able to understand the general behaviour of the response at a constant Re.

The curve for $Re = 9600$ does not have enough data points to reveal a local peak of VIV at $f_s = f_0$, but the majority of the points fall within the first regime between the resonances, where VIV is gradually losing its influence to WIV. In our experiment with varying Re we have noticed that the amplitude of response generally presents a positive slope in this first regime; this is verified now for a constant Re as well. As we have discussed above, Hover & Triantafyllou (2001) also found increasing response

for a constant Re in this regime. Our data agree with theirs in showing a build-up of response between $f_s = f_0$ and $f_w = f_0$. Such an effect is also observed for our curve at $Re = 19\,200$.

Let us move on to the other curves at $Re = 14\,500$ and $19\,200$ that cross $f_w = f_0$ and enter the second regime where WIV dominates. Now that the wake stiffness is greater than the spring stiffness we see that the response is not influenced by reduced velocity anymore, but presents a rather constant level of amplitude for each fixed value of Re. Even if the reduced velocity is increased from 20 to 35 the amplitude of response seems not to be much affected and the data points appear to follow the same trend as long as Re is kept constant. Going back to the curve without springs in figure 8 we are able to find a displacement amplitude for each of our Re curves at $U/Df_0 = \infty$ towards which the data points should be converging. We note that they are slightly higher than the level of amplitude the curves are reaching beyond $f_w = f_0$, but we have to remember that we are still operating with springs, although soft ones, that might be contributing to reduce the response away from the resonance lines.

While on the one hand the VIV peak at $f_s = f_0$ seems to always reach $\hat{y}/D$ around 1.0 (for this value of $m^*\zeta$), the amplitude at the end of the first regime, at $f_w = f_0$, varies with the intensity of the wake-stiffness effect. Because k_w increases with Re the amplitude at $f_w = f_0$ must also increase with Re. This level of amplitude is already very close to the asymptotic value predicted by the experiments without springs; hence, as the spring stiffness gets less important beyond $f_w = f_0$, we expect the curves to be converging towards the values plotted at $U/Df_0 = \infty$.

This series of experiments at constant Re proved that while the response below $f_w = f_0$ is dependent on both Re and reduced velocity, the response for $f_w > f_0$ is clearly governed by Re only. In other words, we conclude that in the first regime where both VIV and WIV are competing (or cooperating) the response increases due to a combination of spring and wake-stiffness effects. Even with constant Re we note a build-up of response while the ratio between k and k_w makes reduced velocity an important parameter. But once the wake stiffness becomes dominant over the springs the response is not affected by the structural stiffness and is only governed by wake stiffness. Now this second regime is clearly dominated by a Reynolds number effect.

7.2. *Equivalent damping*

Another way to comprehend the behaviour of the amplitude of response is to think in terms of an equivalent damping ratio. We can define ζ by the ratio between c and a critical damping:

$$\zeta = \frac{c}{4\pi f_0 m}. \tag{7.1}$$

Note that the natural frequency and the mass of the system are present in the denominator. Apart from removing the pair of springs we keep exactly the same set-up from previous experiments, therefore we assume all other parameters are kept constant including the structural damping c. In other words, we presuppose the friction in the air bearings was kept the same; hence the system would dissipate the same amount of energy for a similar velocity of the cylinder. However, now that the springs are removed we do not have f_0 that can be used to non-dimensionalize ζ as expressed in (7.1).

Govardhan & Williamson (2002) encountered a similar problem to define a suitable damping ratio when performing experiments with a cylinder mounted on air bearings without springs. They also wanted to investigate the VIV response for $U/Df_0 \to \infty$

and achieved that by removing the springs from the elastic system, making $k = 0$ and $f_0 = 0$. In their experiment f followed the shedding frequency throughout the oscillatory regime, therefore they employed an equivalent damping ratio non-dimensionalized by f_s instead of f_0. But in the present WIV investigation f was observed not to follow f_s; instead it increases linearly with flow speed following f_w – the natural frequency given by wake stiffness – as demonstrated above. Therefore, unlike in Govardhan & Williamson (2002), it does not make sense to define an equivalent damping ratio based on the shedding frequency f_s, but based it on the oscillation frequency $f = f_w$ instead:

$$\zeta_w = \frac{c}{4\pi f_w m}. \tag{7.2}$$

According to this definition of ζ_w the damping ratio varies with flow speed since f_w is also varying with U, as seen in (6.6). The same occurred for Govardhan & Williamson (2002), where their damping ratio was based on f_s which also varies with U according to the Strouhal law. (This was not the case with the traditional ζ, which is invariant with U given a constant natural frequency f_0 defined by structural stiffness.) Now, substituting c from (7.2) into (6.3) results in

$$\frac{\hat{y}}{D} = \frac{1}{4\pi}\hat{C}_y \sin\phi \left(\frac{U}{Df}\right)^2 \left(\frac{1}{m^*\zeta_w}\right), \tag{7.3}$$

with a combined $m^*\zeta_w$ parameter appearing in the denominator.

We now observe that the amplitude of response should be inversely proportional to this new $m^*\zeta_w$. However, now the combined mass-damping parameter is not constant but incorporates a variation with flow speed. Because f_w increases with Re, ζ_w decreases with flow speed and, thinking about an equivalent damping term, we reach the same conclusion that the response should in fact increase with Re.

8. Wake stiffness for other separations

Now that we have analysed the WIV response for a pair of cylinders at $x_0/D = 4.0$ we can bring the wake-stiffness concept back to our starting point and investigate the effect it has on other separations. We already know that moving the second cylinder farther downstream does not affect the wake formed in the gap, i.e. the upstream vortex shedding process is not affected if the separation changes from $x_0/D = 4.0$ up to 20.0, the highest case investigated in the present work.

The development of a von Kármán wake from a static cylinder has been diligently studied in the literature. Schaefer & Eskinazi (1958) performed experiments in a wind tunnel in order to model the effect of fluid viscosity in diffusing a vortex from the instant it is shed from the cylinder. The core of concentrated circulation expands with time as vortices travel downstream towards the second body, so if the cylinder is farther away we expect weaker vortices (at least with less concentrated vorticity) to reach that specific position of the wake. Weaker vortices induce weaker fluid forces, therefore we would expect both wake-stiffness and vortex-impulse terms to decrease with increasing x_0.

Looking back at the steady lift map presented in figure 6 we see that the maximum $\overline{C}_y$ is indeed decreasing for larger separations, consequently $\Delta_{\overline{C}_y}$ is also reduced with increases in x_0. To a certain extent it is straightforward to think that the wake-stiffness effect is inversely proportional to x_0 and results in lower values of $f_w D/U$ for larger separations. As a consequence, the frequency of oscillation should also be reduced.

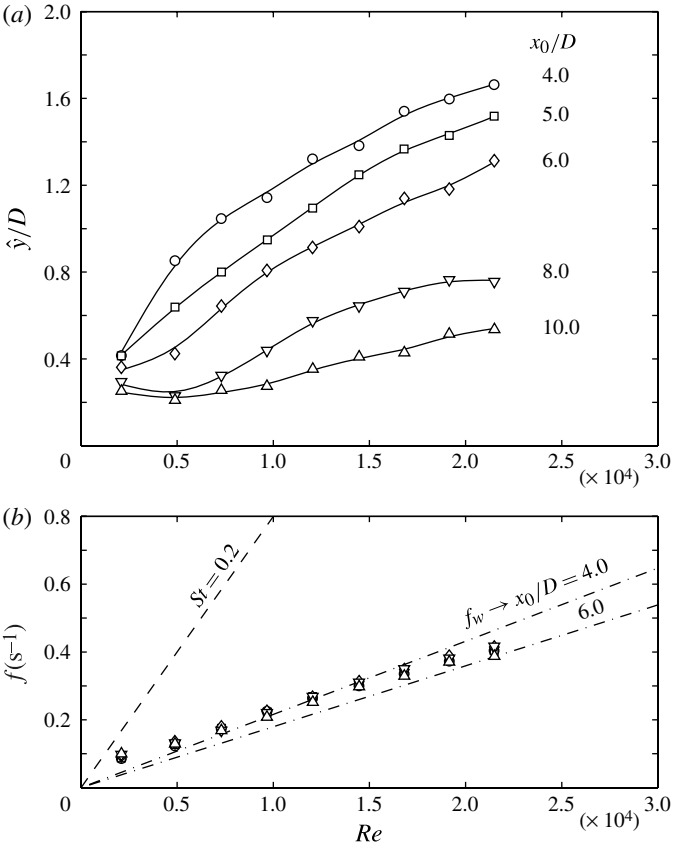

FIGURE 14. WIV response of a downstream cylinder mounted without springs at various x_0 separations: (*a*) displacement; (*b*) dominant frequency of oscillation.

However, (6.3) tells us that the amplitude must increase if fD/U is reduced and all other terms are kept constant. This is clearly not observed in the response with springs presented in figure 4. Instead $\hat{y}/D$ for the WIV regime is seen to be reduced with increasing x_0, up to a separation where no effect from the upstream wake can be sensed by the downstream cylinder and it returns to a simple VIV regime. Therefore, some other non-dimensional terms in (6.3) must be dominating over the effect of fD/U to reduce the response as x_0 is increased.

Figure 14 presents the effect of x_0 on the response of a cylinder mounted without springs. In accordance with (6.3), the amplitude of displacement should increase with Reynolds number for a fixed separation, while $\hat{y}/D$ should be reduced for larger separations if Re is kept constant. Although this plot is not as densely populated with data points as figure 4, it can still reveal the overall behaviour of the response in relation to Re and x_0. The main difference now is that no VIV resonance peak is identified because the system lacks any f_0 conferred by springs, but still the WIV response seems to diminish as the second cylinder is moved farther downstream.

Remember that every point in figure 14 represents an infinite reduced velocity. Therefore, variations observed in the curves are an effect of Re and x_0 only. We can pick one data point from each x_0/D curve at $Re = 2.3 \times 10^4$ in figure 14 and plot

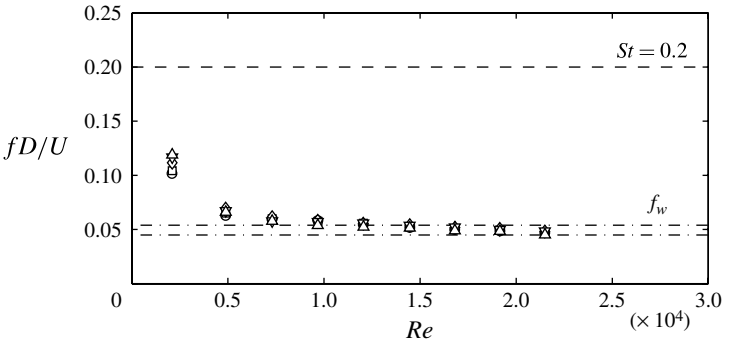

FIGURE 15. Non-dimensionalized dominant frequency of oscillation of a downstream cylinder mounted without springs at various x_0 separations. See figure 14 for key.

them back in figure 4 at $U/Df_0 = \infty$. Every point plotted there (on the right-hand axis) represents the asymptotic value the response would reach if Re were kept constant beyond the vertical dashed line of $Re = 2.3 \times 10^4$. This agreement confirms that beyond the flow speed range in which VIV is important reduced velocity has no effect on the WIV response and the cylinder is expected to sustain a constant level of vibration for the rest of the Re range. It is also verified that the asymptotic value that limits $\hat{y}/D$ is indeed a function of Re and x_0 alone and must be related to the actual configuration of the wake at those conditions.

As we saw in figure 8 for $x_0/D = 4.0$ the frequency of oscillation shows a fairly linear behaviour with Re, which is represented by a constant line when plotted non-dimensionally as fD/U in figure 9. Interestingly, we know that as far as the separation is concerned $\Delta_{\overline{C}_y}$ decreases with x_0. However, when this effect is reflected into f_w it seems to cause only a small variation in the frequency of response, making all frequency curves for different x_0 collapse onto each other. A similar result was observed in figure 4 for the response with springs, where, differently from the displacement, f/f_0 did not show much variation with x_0.

Considering our smallest separation of $x_0/D = 4.0$ we saw that the steady lift field generates, to a first approximation, a wake stiffness effect proportional to $\Delta_{\overline{C}_y} = 0.65$ (figure 7). Again we can plot f_w from (6.6) associated with this steady field as a dot-dashed line in figure 14(*b*). However, on moving the second cylinder farther downstream in the wake we saw that $\Delta_{\overline{C}_y}$ is reduced. Considering the maximum separation measured in the $\overline{C}_y$ map of figure 6 we can estimate a wake-stiffness effect proportional to $\Delta_{\overline{C}_y} = 0.45$ for $x_0/D = 6.0$. If we then plot f_w associated with this weaker wake stiffness in figure 14(*b*) we are able to verify that the expected variation of f between both separations is actually rather small. This is made even clearer when the data are plotted in the non-dimensional form of fD/U in figure 15.

Turning back to our analysis of (6.3) regarding separation, we conclude that the variation of fD/U versus x_0 may be rather small and unlikely to dominate over other non-dimensional groups, leaving us with the vortex-impulse term $\hat{C}_y \sin\phi$ that might present some significant variation with x_0.

As suggested above, the diffusion of vortices in the wake may be responsible for the reduction of the wake stiffness effect observed in figure 6. But, since we argue that

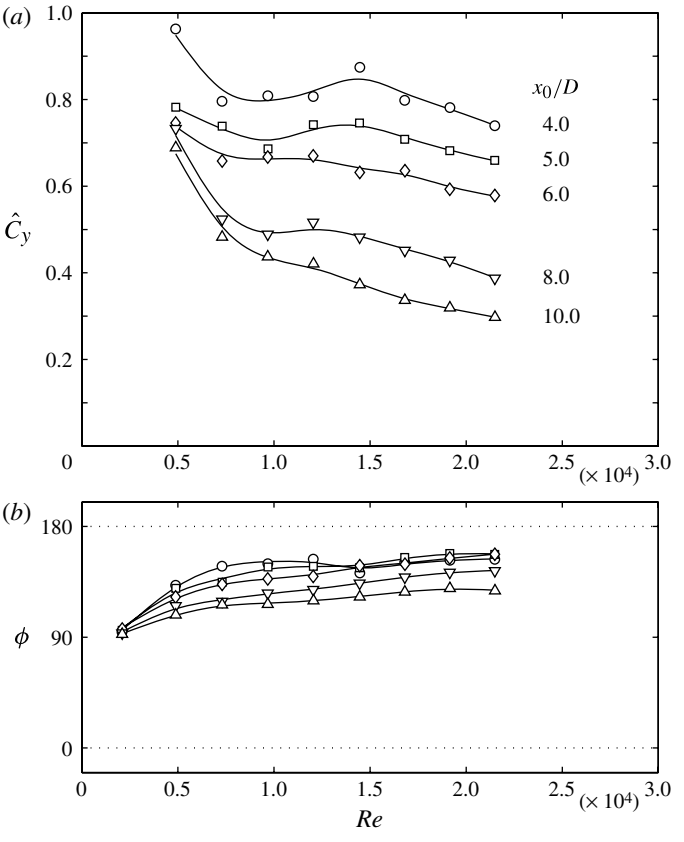

FIGURE 16. Fluctuating lift coefficient (*a*) and phase angle (*b*) for WIV responses without springs at various x_0 separations.

both wake-stiffness and vortex-impulse terms originate in the same phenomenon, we believe that vortex diffusion may also be responsible for changes in $\hat{C}_y \sin\phi$ versus x_0.

Figure 16 presents the variation of $\hat{C}_y$ and ϕ with both Re and x_0. We have shown that $\hat{C}_y$ has a small dependence on Re, resulting in a mildly decreasing slope for $x_0/D = 4.0$. However, as separation is increased in figure 16 we observe that not only is the overall level of $\hat{C}_y$ reduced, but also that the negative slope with Re is accentuated. On the other hand, figure 16(*b*) shows that although ϕ is roughly constant with Re it is also reduced for larger x_0. Now, depending on the combination of both terms, $\hat{C}_y \sin\phi$ can show significant variation with x_0, as much as to dominate over fD/U and govern the behaviour of the response versus separation.

9. Conclusions

The experiment without springs was crucial in the understanding of the WIV phenomenon. It not only revealed the existence of a dominant wake-stiffness effect that can sustain vibrations even if springs are removed, but also helped to explain different regimes of the response when springs are present. We proved that $\overline{C}_y$ towards

the centreline not only provides some restoration for a quasi-static system but is in fact responsible for the characteristic WIV response of a cylinder that is free to vibrate.

The wake-stiffness concept does not explain the excitation mechanism but it predicts rather well the characteristic signature of the WIV response both in terms of displacement and frequency. We can say that while unsteady vortex–structure interactions provide the energy input to sustain the vibrations (Assi *et al.* 2010), it is the wake-stiffness phenomenon that defines the character of the WIV response.

We conclude that the restoration force provided by wake stiffness is strong enough to balance the flow excitation and produce oscillatory motion for a system without structural stiffness. The cylinder was not observed to drift away from the centreline, but presented WIV throughout the *Re* range of the experiments. The analytical modelling for a system without springs revealed that the amplitude of response should increase with Reynolds number. This was verified by experimental data. However, a simple model that did not account for nonlinear effects in the fluid force was not able to predict the correct level of amplitude. We found that the WIV response should converge to an asymptotic value that depends on *Re* but not on reduced velocity.

As $\hat{y}/D$ is increased beyond a certain limit, the cylinder starts to reach amplitudes outside the wake interference region. The wake-stiffness effect cannot be represented by a linear spring anymore, but the overall stiffness tends to be reduced. This effect was in agreement with cases with and without springs and also with various x_0 separations. A simple linear model was able to predict the frequency of response rather well. It was confirmed that the cylinder without springs does not respond following the vortex shedding frequency f_s. Instead the response matches the frequency branch f_w associated with wake stiffness, which was well predicted by the model. A cylinder with springs responds with a frequency that combines influences from f_w and f_0, yet is different from both.

In our experiments we observed a gradual transition from an initial VIV regime to a dominating WIV regime as flow speed was increased. The boundaries between them were found to be related to two resonances: $f_s = f_0$ and $f_w = f_0$. The first regime has a clear VIV character, with a local peak of displacement occurring at $f_s = f_0$. The wake stiffness is still smaller than the spring stiffness, making U/Df_0 a significant parameter. The amplitude of the VIV peak is in agreement with the response curve for a single cylinder and showed no noticeable dependence on *Re* for the range of the experiments. The second regime is characterized by an established WIV response that experiences no influence of VIV. Beyond $f_w = f_0$ the wake-stiffness effect is dominant over the spring stiffness and reduced velocity becomes irrelevant.

During the transition between the regimes we find an intermediate condition in which VIV is losing strength and WIV is taking control. Between the resonances $f_s = f_0$ and $f_w = f_0$ the response leaves the VIV peak until it reaches a characteristic value at $f_w = f_0$ that is dependent on *Re*. During the transition, reduced velocity gradually loses its influence until the WIV response is only dominated by *Re* as it enters the second regime. The total stiffness of the system is not only caused by either the wake stiffness (k_w) or the spring stiffness (k) alone, but it is a combination of both; k is very relevant in the first regime, but k_w becomes dominant in the second. Nevertheless, both k and k_w contribute in part to the characteristic displacement and frequency responses.

As expected, the x_0 separation between the two cylinders was confirmed to have a significant effect on the response. We suggest this effect is related to an increase in vortex diffusion and flow three-dimensionality as the gap is enlarged. The WIV response changed as the second cylinder was moved farther downstream. The first VIV

regime experienced no influence of x_0 and the local resonance peak kept the same level of displacement for all separations between $4D$ and $20D$. On the other hand, the second WIV regime showed a strong influence of the separation. The characteristic WIV branch of response gradually disappeared with increasing x_0 until the response resembled only that of a typical VIV phenomenon. In contrast with the displacement, the frequency of oscillation showed only a small variation with x_0, with curves for all separations collapsing onto the value predicted by the wake-stiffness effect, especially for the case without springs. Such a strong x_0 dependence was associated with the fact that vortices from the upstream cylinder have more time to diffuse as they travel to reach a cylinder located farther downstream. Together with that is the fact that increasing three-dimensionality of the flow also weakens the coherent wake. Weaker vortices induced weaker forces. Both the wake-stiffness effect (proportional to $\Delta_{\overline{C}_y}$) and the vortex-impulse term (related to $\hat{C}_y \sin\phi$) are affected.

By modelling a second-order oscillator without springs but incorporating the stiffness as a consequence of the fluid force (wake stiffness) we were able to predict the frequency behaviour rather well. But no matter how good this approach was in regard to the frequency response, the displacement response is somewhat more complex and is not fully captured by this first approximation. We believe this is due to the simplicity in modelling the term $\hat{C}_y \sin\phi$. Even though in some analysis we have considered $\hat{C}_y$ and ϕ to be independently related to the wake-stiffness and vortex–impulse terms, we are fully aware that this decomposition is not ideal and must overlook significant secondary effects.

A simple harmonic model such as the one we have employed cannot account for nonlinear effects that might be important to the system. It will not be able, for example, to predict the asymptotic effect that is limiting the displacement. The complex interaction between body and wake causes $\Delta_{\overline{C}_y}$ and $\hat{C}_y \sin\phi$ to be coupled in such a way that we cannot simply analyse them independently. Since we believe both wake-stiffness and vortex-impulse terms originate in the same fluid-mechanic phenomenon, we are not able to uncouple and isolate their effects into linear concepts. We argue that an improved, nonlinear model is necessary to account for more complex fluid-dynamic phenomena that we have identified to exist but were not considered in our model.

In Assi *et al.* (2010) we have discussed the idea that WIV could not be predicted by the classical galloping theory. Remember that, in the literature, WIV had been referred to as a type of galloping mostly because the typical response presents a build-up of amplitude for higher reduced velocities. But now we know that the response is increasing due to the wake-stiffness effect as a function of Reynolds number. We have argued that quasi-steady assumptions commonly employed by the classical galloping theory would not fit the WIV phenomenon nor help to understand the real flow–structure mechanism. For that reason we have insisted on a dissociation of WIV from the classical galloping idea. In the present work we have shown that WIV is indeed a wake-dependent type of flow-induced vibration. Remember that according to the classical galloping theory the oscillations of the body are dependent on the structural stiffness of the system to provide the restoration force, even more for the wake-flutter phenomenon of interfering cylinders, where structural stiffness in 2-dof is required. In our case, however, we showed that a body without any structural stiffness can be excited into flow-induced vibration. If some stiffness is provided by the flow, the body is able to be excited and sustained into oscillatory motion. The concept of wake stiffness is a powerful one but it also requires the existence of an unsteady

vortex wake present in the gap to generate the excitation. Therefore we continue to propose that WIV is not to be understood as a type of classical galloping, but must be interpreted as a wake-excited and wake-sustained FIV mechanism.

Acknowledgements

G.R.S. and B.S.C wish to thank CAPES, Brazilian Ministry of Education, for their PhD scholarships. J.R.M. is grateful to CNPq for a research scholarship.

REFERENCES

ASSI, G. R. S. 2009 Mechanisms for flow-induced vibration of interfering bluff bodies. PhD thesis, Imperial College London, London, UK. available from www.ndf.poli.usp.br/∼ gassi.

ASSI, G. R. S., BEARMAN, P. W. & MENEGHINI, J. R. 2010 On the wake-induced vibration of tandem circular cylinders: the vortex interaction excitation mechanism. *J. Fluid Mech.* **661**, 365–401.

ASSI, G. R. S., MENEGHINI, J. R., ARANHA, J. A. P., BEARMAN, P. W. & CASAPRIMA, E. 2006 Experimental investigation of flow-induced vibration interference between two circular cylinders. *J. Fluids Struct.* **22**, 819–827.

BEARMAN, P. W. 1984 Vortex shedding from oscillating bluff bodies. *Annu. Rev. Fluid Mech.* **16**, 195–222.

BLEVINS, R. D. 1990 *Flow-Induced Vibration*, 2nd edn. Van Nostrand Reinhold.

BOKAIAN, A. & GEOOLA, F. 1984 Wake-induced galloping of two interfering circular cylinders. *J. Fluid Mech.* **146**, 383–415.

BRIKA, D & LANEVILLE, A. 1999 The flow interaction between a stationary cylinder and a downstream flexible cylinder. *J. Fluids Struct.* **13**, 579–606.

GOVARDHAN, R. & WILLIAMSON, C. H. K. 2002 Resonance forever: existence of a critical mass and an infinite regime of resonance in vortex-induced vibration. *J. Fluid Mech.* **473**, 147–166.

HOVER, F. S. & TRIANTAFYLLOU, M. S. 2001 Galloping response of a cylinder with upstream wake interference. *J. Fluids Struct.* **15**, 503–512.

IGARASHI, T. 1981 Characteristics of the flow around two circular cylinders arranged in tandem. *Bull. Japan Soc. Mech. Engrs* **24**, 323–331.

KHALAK, A. & WILLIAMSON, C. H. K. 1999 Motions, forces and mode transitions in vortex-induced vibrations at low mass-damping. *J. Fluids Struct.* **13**, 813–851.

KING, R. & JOHNS, D. J. 1976 Wake interaction experiments with two flexible circular cylinders in flowing water. *J. Sound Vib.* **45**, 259–283.

LANEVILLE, A. & BRIKA, D. 1999 The fluid and mechanical coupling between two circular cylinders in tandem arrangement. *J. Fluids Struct.* **13**, 967–986.

MORSE, T. L. & WILLIAMSON, C. H. K. 2009 Prediction of vortex-induced vibration response by employing controlled motion. *J. Fluid Mech.* **634**, 5–39.

NORBERG, C. 1998 LDV-measurements in the near wake of a circular cylinder. In *Advances in Understanding of Bluff Body Wakes and Flow-Induced Vibration* (ed. C. H. K. Williamson & P. W. Bearman). pp. 1–12. ASME.

PARKINSON, G. V. 1989 Phenomena and modelling of flow-induced vibrations of bluff bodies. *Prog. Aeronaut. Sci.* **26**, 169–224.

PRICE, S. J. 1975 Wake-induced flutter of power transmission conductors. *J. Sound Vib.* **38**, 125–147.

PRICE, S. J. 1976 The origin and nature of the lift force on the leeward of two bluff bodies. *Aeronaut. Q.* **26**, 1154–1168.

RUSCHEWEYH, H. P. 1983 Aeroelastic interference effects between slender structures. *J. Wind Engng Ind. Aerodyn.* **14**, 129–140.

SARPKAYA, T. 1979 Vortex-induced oscillations, a selective review. *J. Appl. Mech.* **46**, 241–258.

SCHAEFER, J. W. & ESKINAZI, S. 1958 An analysis of the vortex street generated in a viscous fluid. *J. Fluid Mech.* **6**, 241–260.

WILLIAMSON, C. H. K. & GOVARDHAN, R. 2004 Vortex-induced vibrations. *Annu. Rev. Fluid Mech.* **36**, 413–455.

ZDRAVKOVICH, M. M. 1974 Flow-induced vibrations of two cylinders in tandem and their suppression. In *International Symposium of Flow Induced Structural Vibrations* (ed. E. Naudascher). pp. 631–639. Springer.

ZDRAVKOVICH, M. M. 1977 Review of flow interference between two circular cylinders in various arrangements. *Trans. ASME: J. Fluids Engng* **99**, 618–633.

ZDRAVKOVICH, M. M. 1985 Flow induced oscillations of two interfering circular cylinders. *J. Sound Vib.* **101**, 511–521.

ZDRAVKOVICH, M. M. 1988 Review of interference-induced oscillations in flow past two circular cylinders in various arrangements. *J. Wind Engng Ind. Aerodyn.* **28**, 183–200.

ZDRAVKOVICH, M. M. 1997 *Flow Around Circular Cylinders*, vol. 1. 1st edn. Oxford University Press.

ZDRAVKOVICH, M. M. & MEDEIROS, E. B. 1991 Effect of damping on interference-induced oscillations of two identical circular cylinders. *J. Wind Engng Ind. Aerodyn.* **38**, 197–211.